How to study water-rock-gas interactions at elevated T-P?

An experimental overview

Laurent Truche

laurent.truche@univ-grenoble-alpes.fr

June 20th 2019 – High Pressure School, ESRF, Grenoble

ISTerre
Institut des Sciences de la Terre

cnrs
dépasser les frontières

UNIVERSITÉ
Grenoble
Alpes



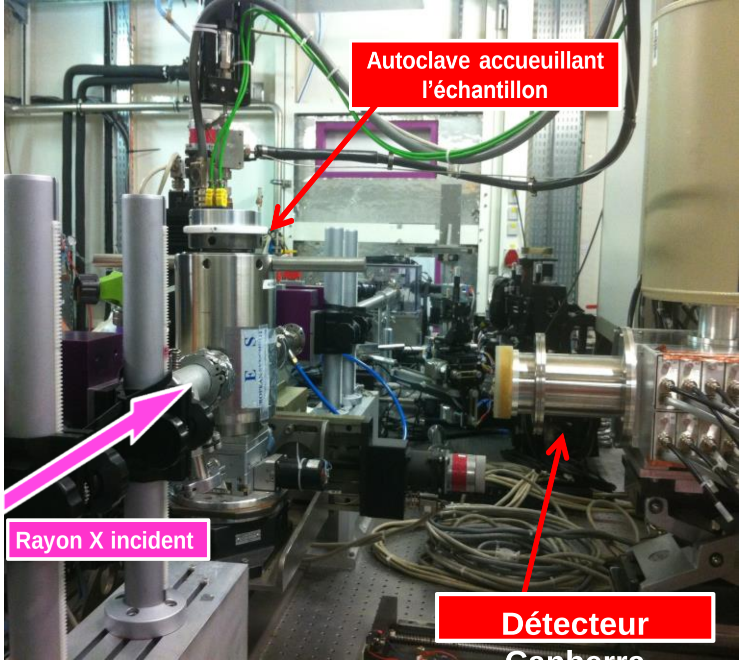
Autoclave accueillant l'échantillon
Rayon X incident
Détecteur
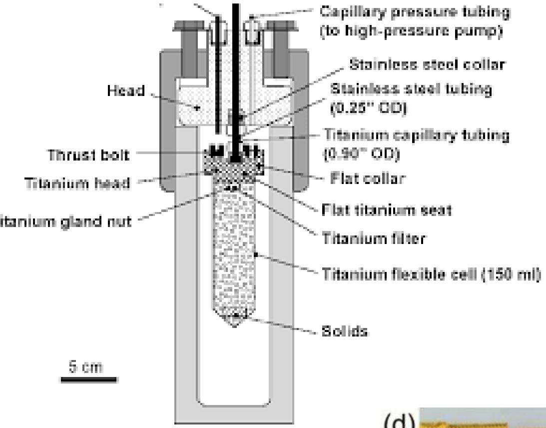
Capillary pressure tubing (to high-pressure pump)
Stainless steel collar
Stainless steel tubing (0.25" OD)
Head
Titanium capillary tubing (0.90" OD)
Thrust bolt
Titanium head
Flat collar
Flat titanium seat
itanium gland nut
Titanium filter
Titanium flexible cell (150 ml)
Solids
5 cm

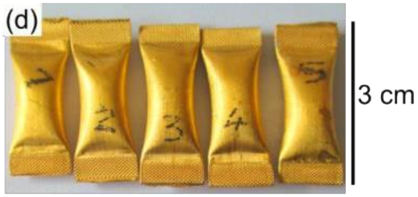
(d)
3 cm
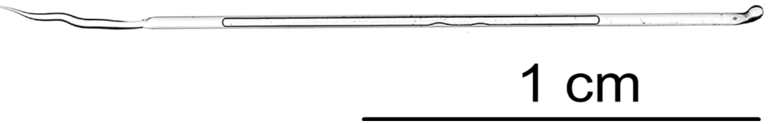
1 cm

How to study water-rock-gas interactions at elevated T-P?

1) Hydrothermal Autoclaves

Sampling at high P-T or Quenching → solubility, total Me concentration

LIMITATION

→ change speciation

→ Precipitation/dissolution during cooling, Colloids formation

→ Degasing

→ pH/redox change

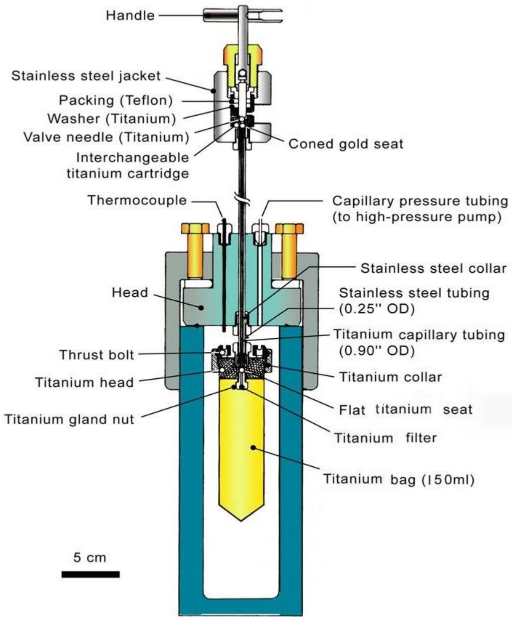

Ti Batch autoclave

Up to 400°C and 300 bar

- → Fluid sampling
- → Gas sampling
- → Post morterm solid analysis
- → May be fitted wi in situ pH and Raman probes

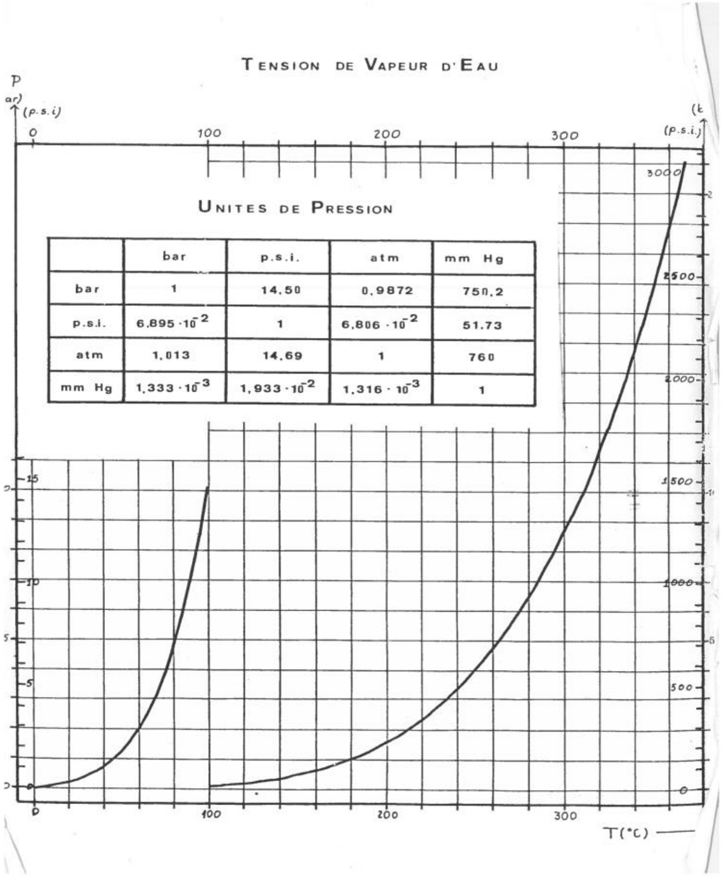

UNITES DE PRESSION

	bar	p.s.i.	atm	mm Hg
bar	1	14,50	0,9872	750,2
p.s.i.	$6{,}895 \cdot 10^{-2}$	1	$6{,}806 \cdot 10^{-2}$	51.73
atm	1,013	14,69	1	760
mm Hg	$1{,}333 \cdot 10^{-3}$	$1{,}933 \cdot 10^{-2}$	$1{,}316 \cdot 10^{-3}$	1

LIQUID VOLUMES AND VAPOR PRESSURES FOR WATER IN A CLOSED VESSEL AT ELEVATED TEMPERATURES

Tx remplis.	Temperature, T °F	Temperature, T °C	Specific Volume of the Liquid cu. ft./lb.	bar	Vapor Pressure psig (gage)	Psat NIST (bar)	Volume Multiplier Sp.V T /Sp.V 77F	Volume Increase %
1	77	25	.01607		—		1.00	0
0.96	212	100	.01672		0	→ 4,76 (150°C)	1.04	4
0.87	392	200	.01853	14,55 =	211	→ 15,55 (200°C)	1.15	15
0.80	482	250	.0201	38,76 =	562	→ 39,76 (250°C)	1.25	25
0.75	540	282	.0215	65,38 =	948	→ 64,16 (280°C)	1.34	34
0.71	572	300	.0225	84,83 =	1230		1.40	40
0.66	610	321	.0241		1650		1.50	50
0.58	660	349	.0278		2350		1.73	73
0.51	685	363	.0315		2780		1.96	96
0.43	700	371	.0369		3070		2.30	130
0.42	702	372	.0385		3120		2.40	140
0.39	704	373	.0410		3160		2.55	155
0.32	705	374 (Critical Point)	.0503		3190		3.13	213

Data from Keenan & Keyes, "Thermodynamic Properties of Steam", John Wiley & Sons, Inc., New York

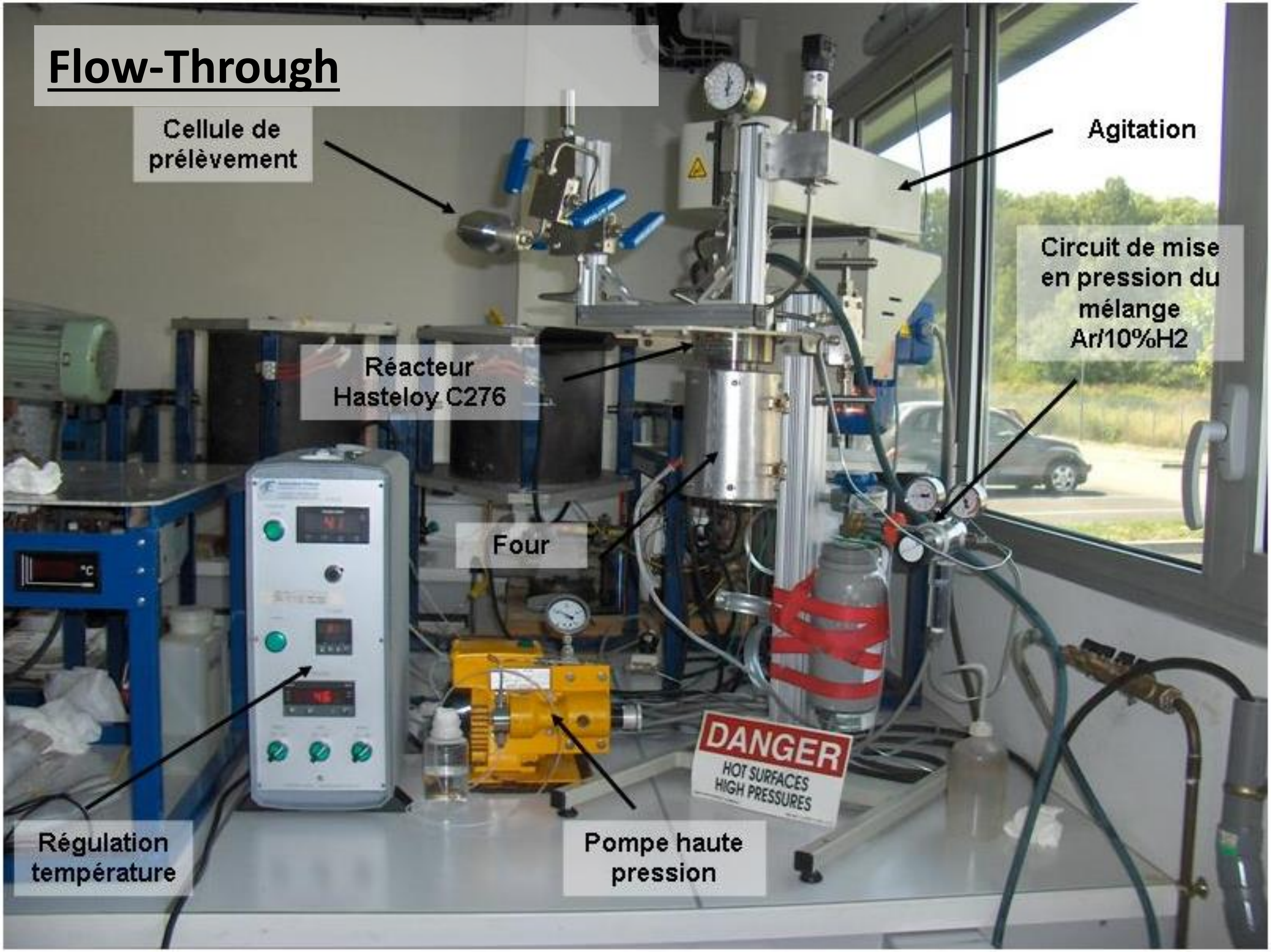
Flow-Through
Cellule de prélèvement
Agitation
Circuit de mise en pression du mélange Ar/10%H2
Réacteur Hasteloy C276
Four
Régulation température
Pompe haute pression
DANGER
HOT SURFACES
HIGH PRESSURES

Solubilities of the assemblage pyrite – pyrrhotite – magnetite – galena – sphalerite in 2.0 and 4.0 molal NaCl and NaBr solutions at 200°C
Crerar et al. (1985), Canadian mineralogist

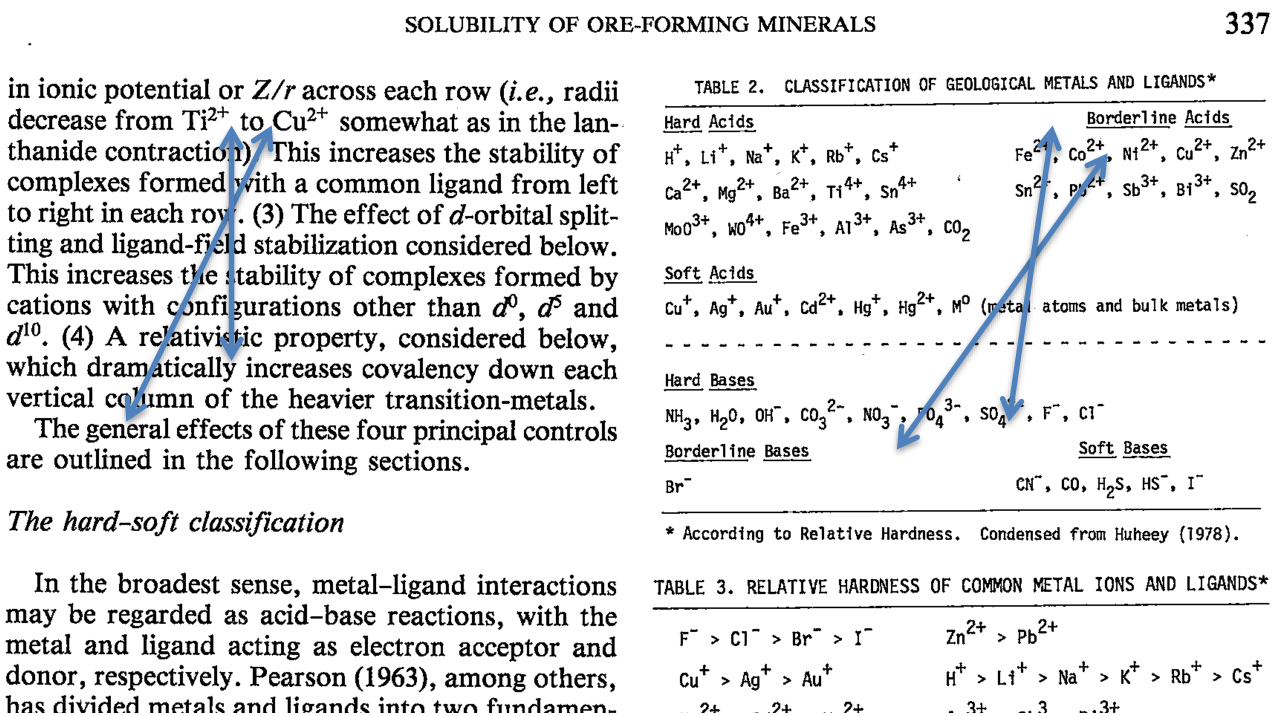

SOLUBILITY OF ORE-FORMING MINERALS 337

in ionic potential or Z/r across each row (*i.e.*, radii decrease from Ti^{2+} to Cu^{2+} somewhat as in the lanthanide contraction). This increases the stability of complexes formed with a common ligand from left to right in each row. (3) The effect of *d*-orbital splitting and ligand-field stabilization considered below. This increases the stability of complexes formed by cations with configurations other than d^0, d^5 and d^{10}. (4) A relativistic property, considered below, which dramatically increases covalency down each vertical column of the heavier transition-metals.

The general effects of these four principal controls are outlined in the following sections.

The hard–soft classification

In the broadest sense, metal–ligand interactions may be regarded as acid–base reactions, with the metal and ligand acting as electron acceptor and donor, respectively. Pearson (1963), among others, has divided metals and ligands into two fundamen-

TABLE 2. CLASSIFICATION OF GEOLOGICAL METALS AND LIGANDS*

Hard Acids: H^+, Li^+, Na^+, K^+, Rb^+, Cs^+, Ca^{2+}, Mg^{2+}, Ba^{2+}, Ti^{4+}, Sn^{4+}, MoO^{3+}, WO^{4+}, Fe^{3+}, Al^{3+}, As^{3+}, CO_2

Borderline Acids: Fe^{2+}, Co^{2+}, Ni^{2+}, Cu^{2+}, Zn^{2+}, Sn^{2+}, Pb^{2+}, Sb^{3+}, Bi^{3+}, SO_2

Soft Acids: Cu^+, Ag^+, Au^+, Cd^{2+}, Hg^+, Hg^{2+}, M^0 (metal atoms and bulk metals)

Hard Bases: NH_3, H_2O, OH^-, CO_3^{2-}, NO_3^-, PO_4^{3-}, SO_4^{2-}, F^-, Cl^-

Borderline Bases: Br^-

Soft Bases: CN^-, CO, H_2S, HS^-, I^-

* According to Relative Hardness. Condensed from Huheey (1978).

TABLE 3. RELATIVE HARDNESS OF COMMON METAL IONS AND LIGANDS*

$F^- > Cl^- > Br^- > I^-$ $\quad$ $Zn^{2+} > Pb^{2+}$

$Cu^+ > Ag^+ > Au^+$ $\quad$ $H^+ > Li^+ > Na^+ > K^+ > Rb^+ > Cs^+$

NaBr

Fe>Pb>Zn

NaCl

Fe>Zn>Pb

→ Pb (soft acid) prefers to complex with the softer Br^-

→ Zn harder acid prefers harder Cl^-

REE solubility in carbonate bearing aqueous solutions under hydrothermal conditions

0.5 mol CO_2 / kg H_2O

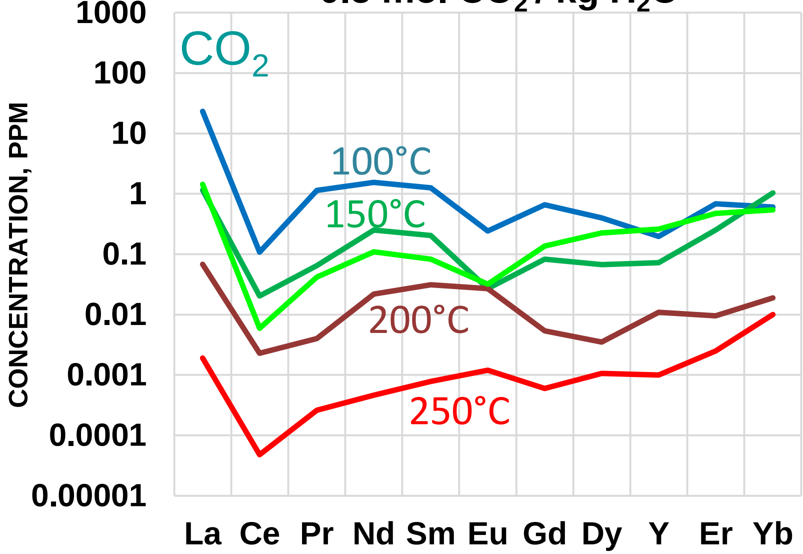

0.5 mol Na_2CO_3 / kg H_2O

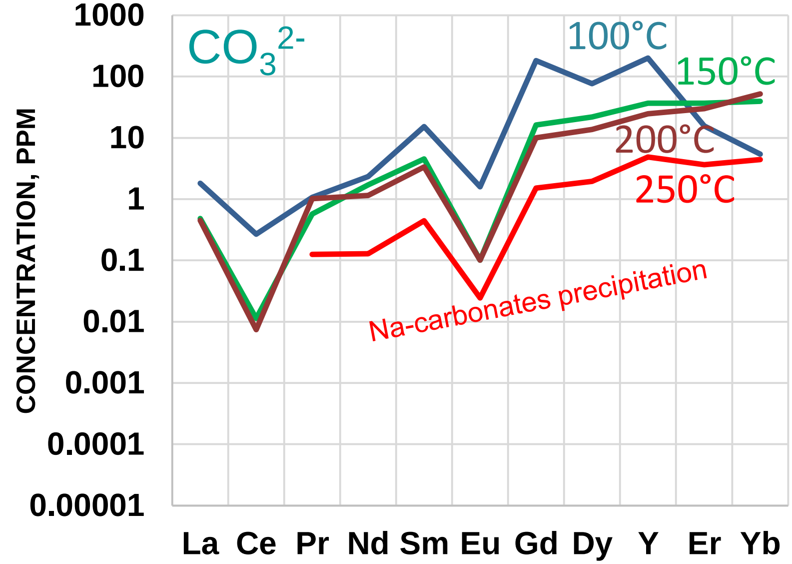

0.5 mol $NaHCO_3$ / kg H_2O

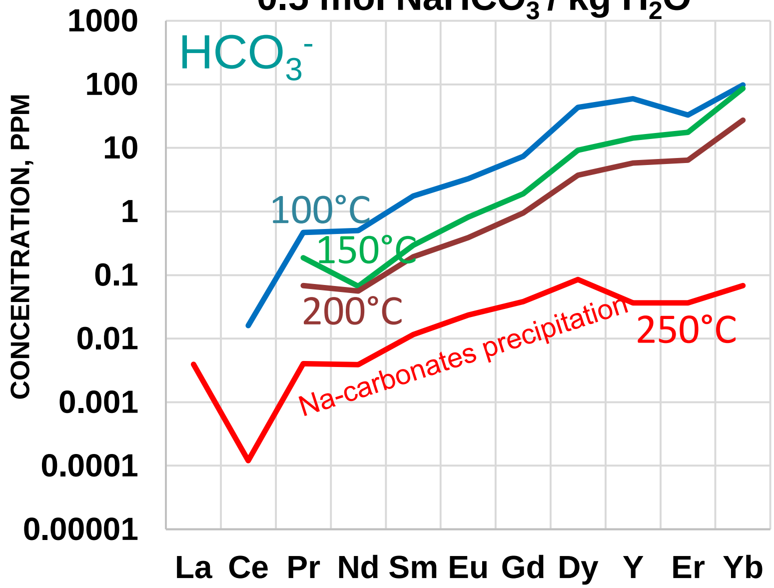

Concentrations of REEs decrease with increasing temperature in all experiments.

Heavy REE are more soluble (~100 ppm) than light REE (<1 ppm) in neutral and alkaline fluids.

Ce-anomaly is present in all experiments.

Eu-anomaly is present only in the experiment with Na_2CO_3.

Kokh et al., in prep

Kinetic of pyrite reduction into pyrrhotite

$FeS_2(s) + (1-x)\ H_2(aq) = FeS_{1+x}(s) + (1-x)\ H_2S(aq) \quad (0<x<0.125)$

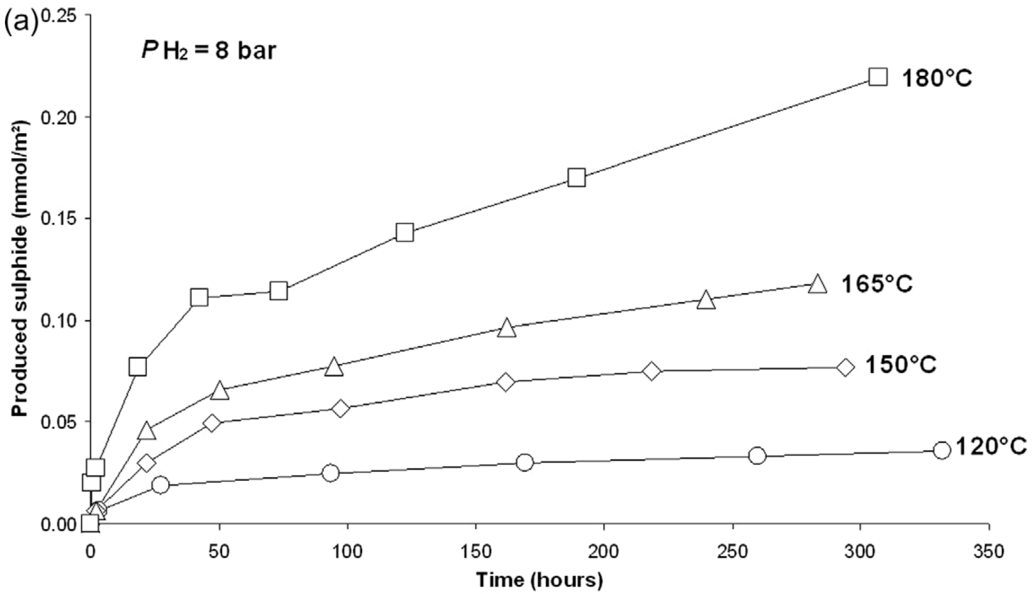

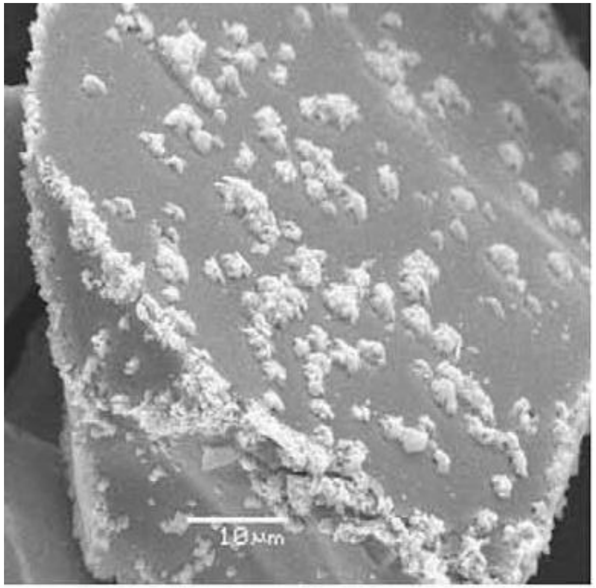

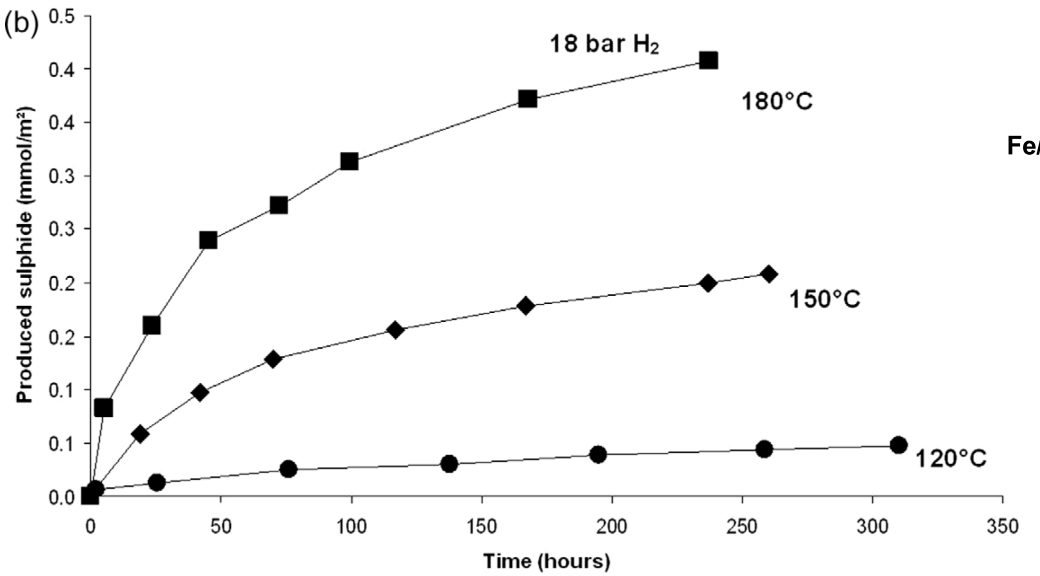

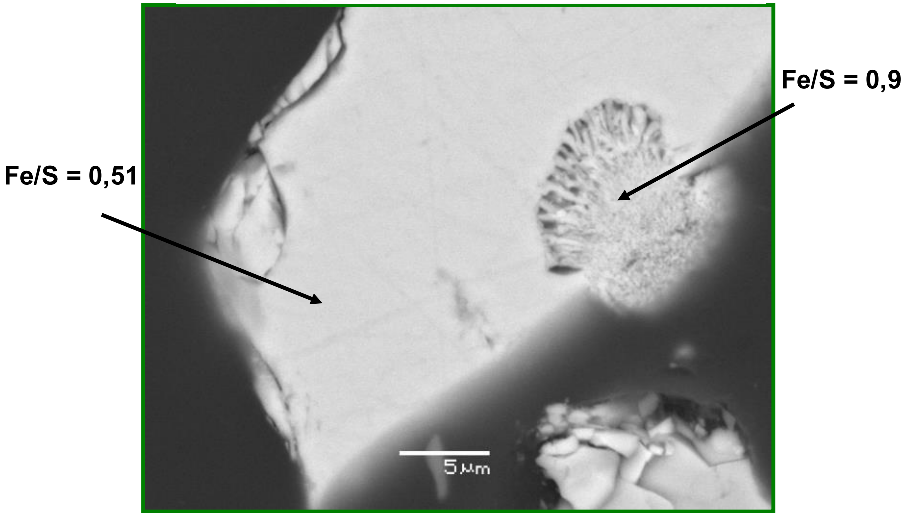

Truche et al., 2010

Flexible-cell rocking autoclave

Up to 500°C and 2 kbar

→ Fluid sampling
→ Gas sampling
→ Post morterm solid analysis

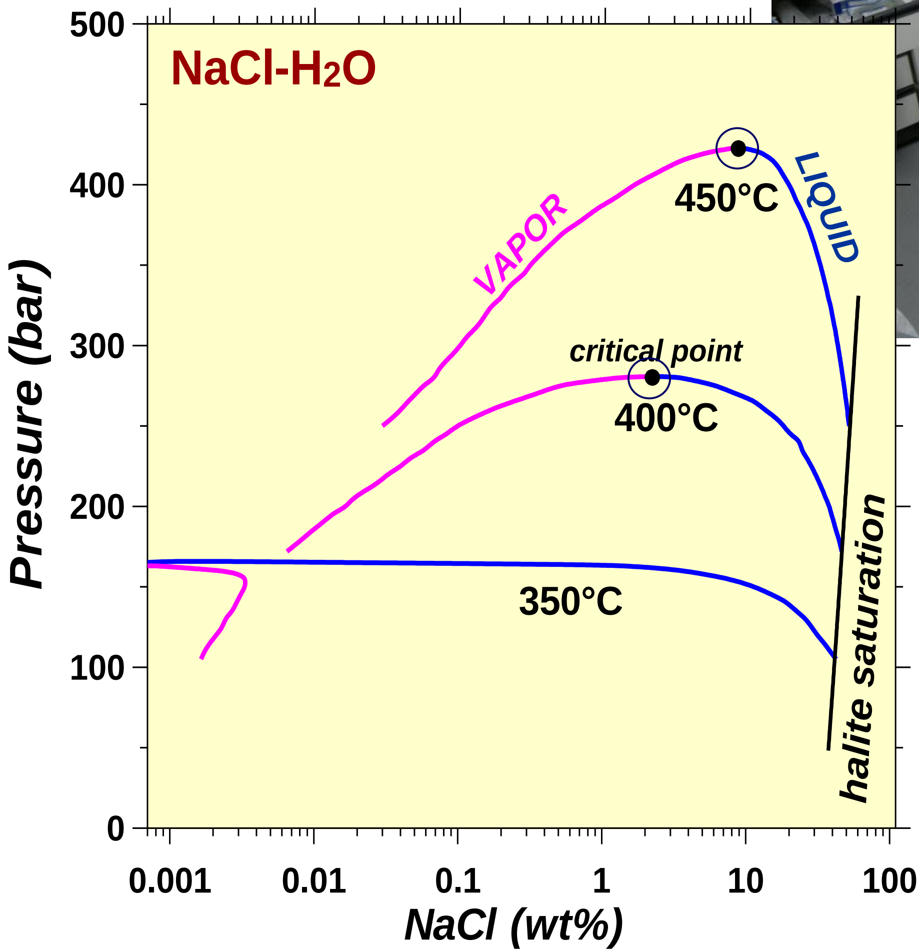

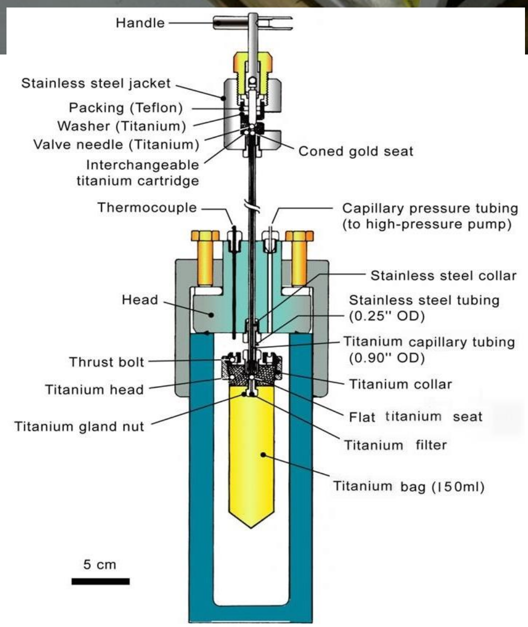

Solubility of CdO and ZnO in pure H_2O

(Coretest reactor)

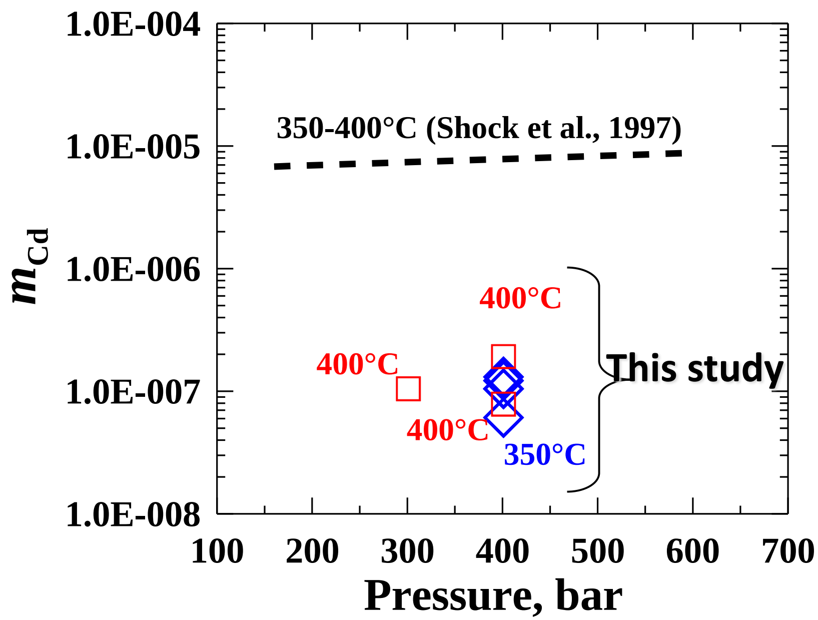

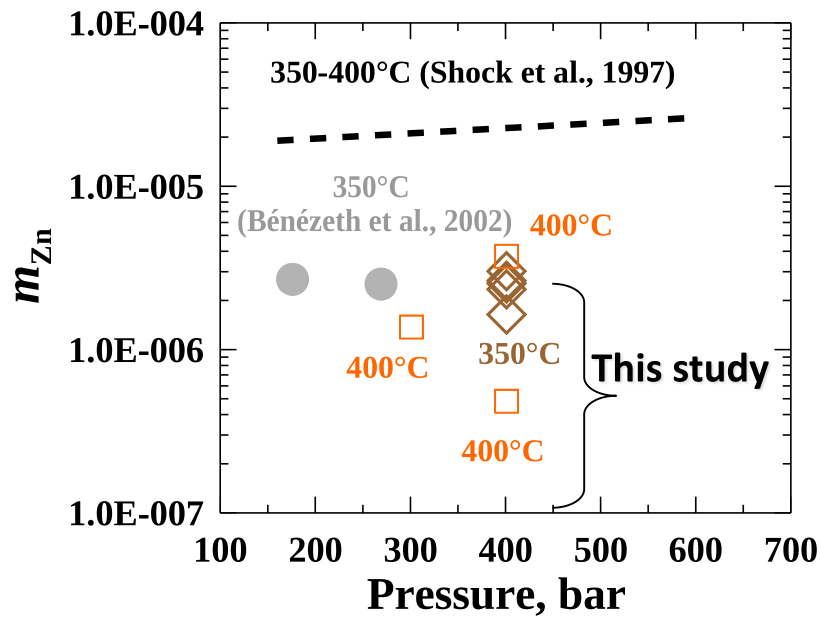

~1 ppb !!!

Cd

~10 ppb !!!

Zn

In hydrothermal fluids the hydroxide complexes of Cd and Zn are very weak !

Bazarkina et al. (2009)

Solubility of CdO and ZnO: effect of chloride

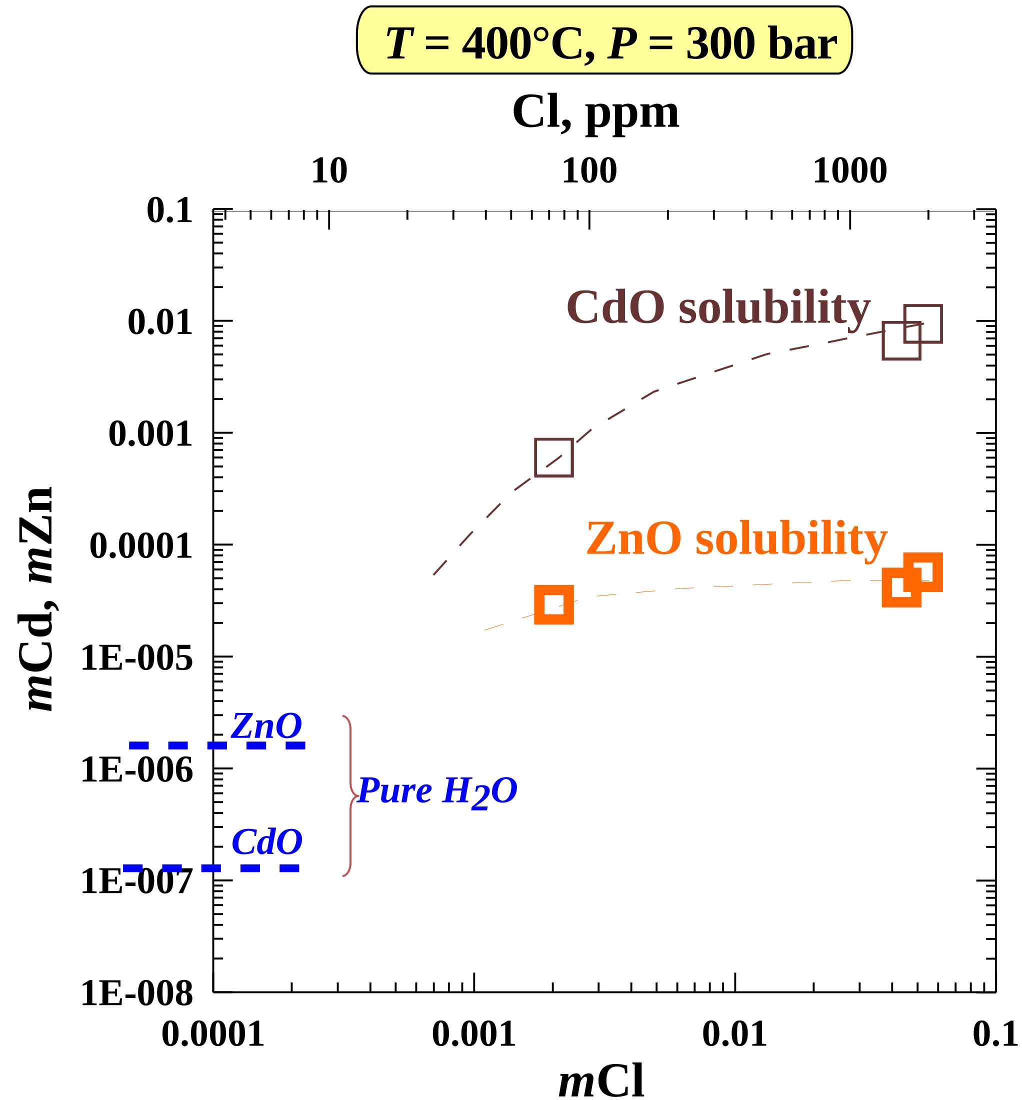

The presence of Cl increases both CdO and ZnO solubility by <u>orders</u> of magnitude !!!!

Peralkaline granite hydrothermal alteration

Kola Peninsula → H_2-bearing gas flowing out of the borehole

Strange Lake pluton (Canada), Ilimaussaq (Greenland), Khibina (Russia)

→ H_2 + hydrocarbons (up to C6) bearing fluid inclusion

Inorganic synthesis of hydrocarbons during alteration of peralkaline granite

and Identification of Species

ıks and standardisation was achieved nounts of known gas mixtures (avail- rom Scott® Speciality Gases Co., ıto the gas chromatograph, except for ected as saturated vapour at known ıre. Blanks were run by crushing inclu- ırtz crystals and pure-silica rods, frag- :leaned exactly as would be regular

eliminated because N_2, as the carrie Ar produces a signal with the inverse extremely low fugacity at the condit study, and the detection limits of CO ... Moreover, as discussed be most favourable conditions for its f >500°C and f_{O_2} < QFM), is unlike >1% of the carbonic species. Figure 2 for analyses of a sample and a blan rier gas.

Salvi and Williams-Jones (1997), Potter et al. (2013)

$$3Na_3Fe^{II}_4Fe^{III}Si_8O_{22}(OH)_{2\,(arfvedsonite)} + 2H_2O$$
$$=$$
$$9NaFe^{III}Si_2O_{6\,(aegirine)} + 2Fe_3O_{4\,(magnétite)} + 6SiO_{2\,(quartz)} + 5H_2$$

Experimental investigations

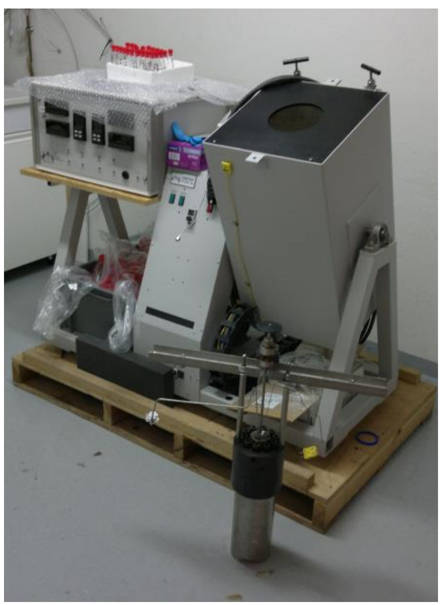

Titanium Autoclave: 280-300°C Psat

5 experiments
- W/R =10
- solids 100-200 micron
- Ar

1. Quartz + H20 → Blank
2. Strange Lake granite + H20
3. Strange Lake granite + 0.01 m HCl
4. Strange lake granite + 0.001m NaOH
5. Strange Lake granite + 0.1m NaCl

Coretest, Ti-Au flexible cell, 350-400°C, 500 bar

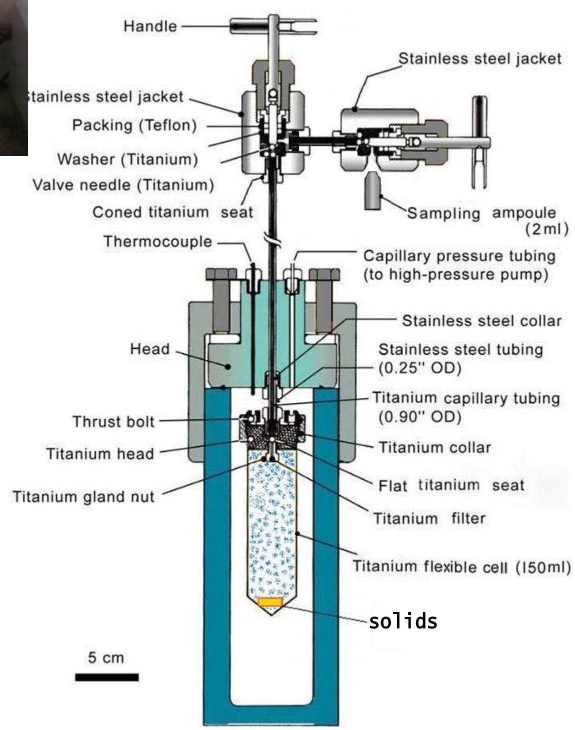

Flexible-cell hydrothermal reactor

1 experiment
- W/R =10
- solids 100-200 micron
- Ar
- H_2O and H_2O-NaCl system

Fluid and gas sampling

Post mortem solid analysis

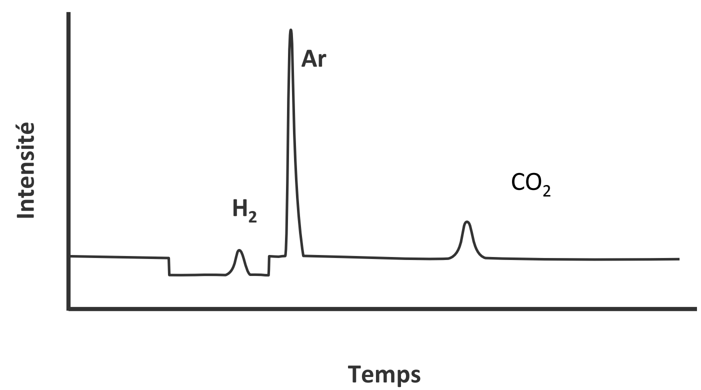

Results : experiments @ 280-300°C and Psat – H_2O + Strange Lake granite

Blank : No H_2 production → Ti is inert and Si-OH site at the Qtz surface do not react to form H_2

Strange Lake granite hydrothermal alteration

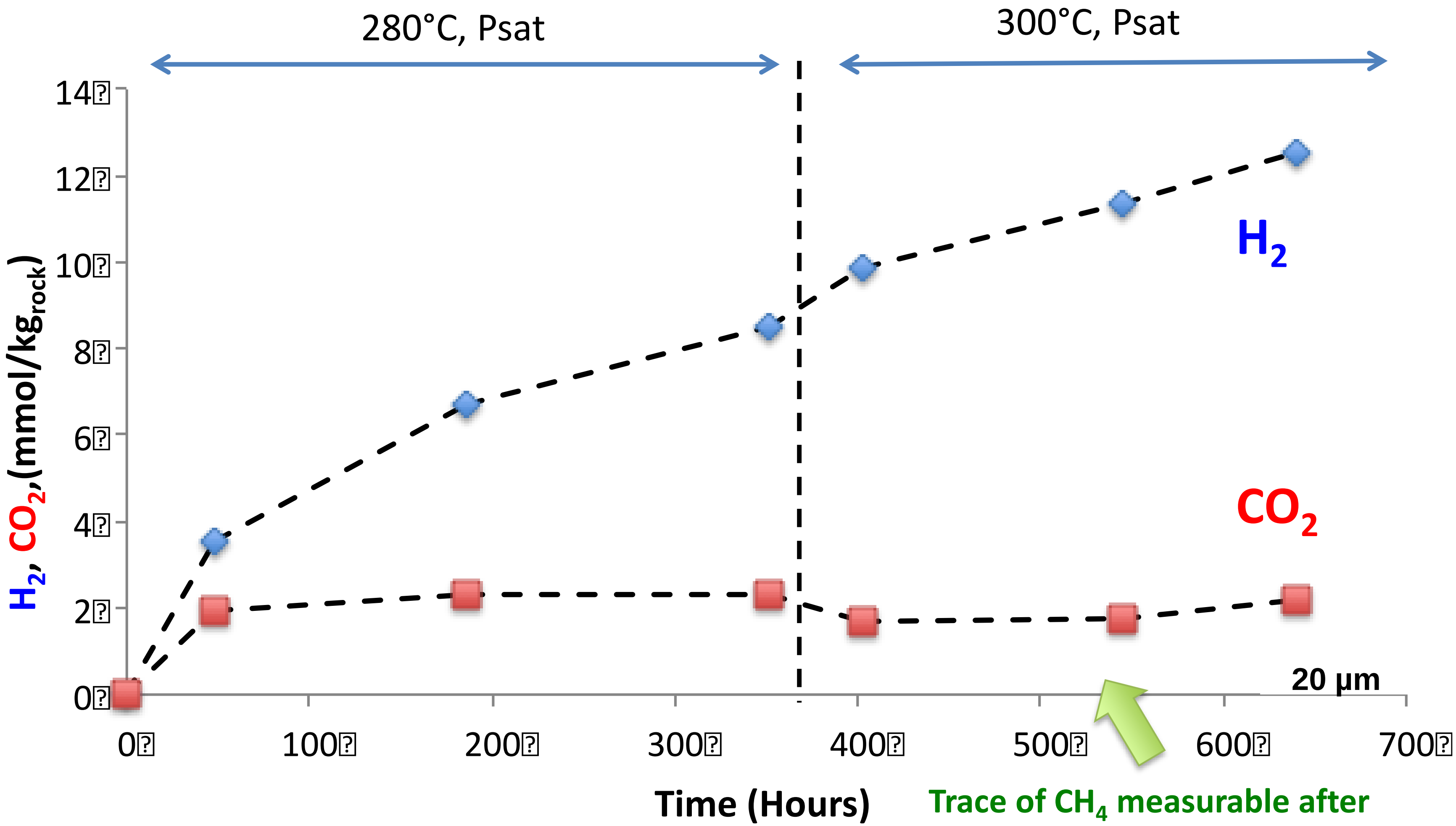

Trace of CH_4 measurable after 500 hrs elapsed time

H_2 generation increases when pH increases

Unreacted arfvedsonite

Arfvedsonite after reaction

$[Na_{3.25}, K_{0.31}][Fe^{2+}_{2.10}, Fe^{3+}_{1.18}, Al_{0.29}][Si_{7.96}, Ti_{0.04}]O_{22}(OH)_2$.

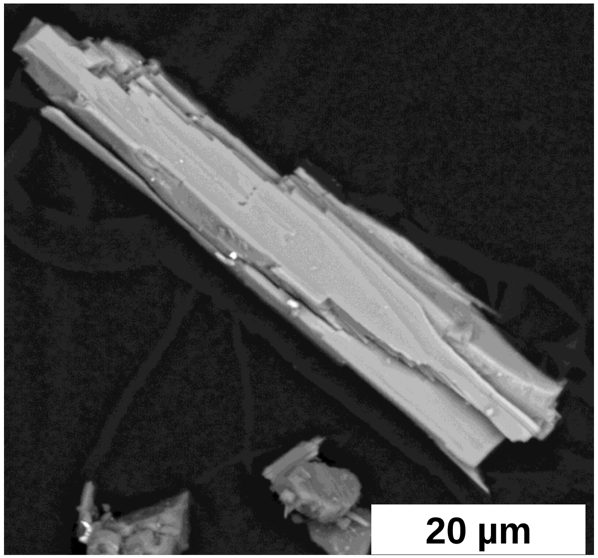

300°C

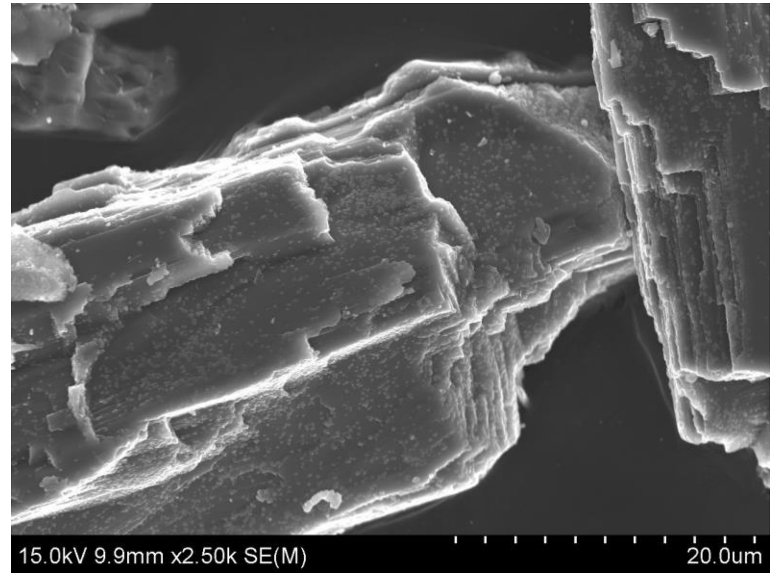

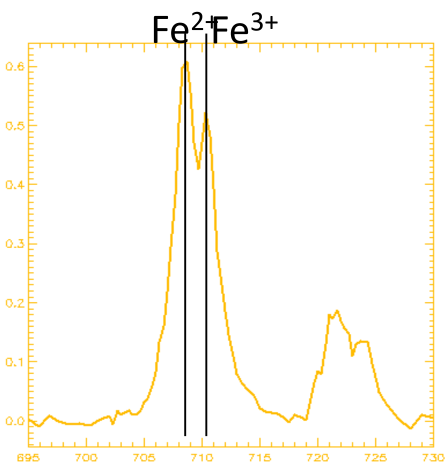

Arfvedsonite « pure »
$Fe^{3+}/\Sigma Fe$ = 31,2 %

STXM-XANES

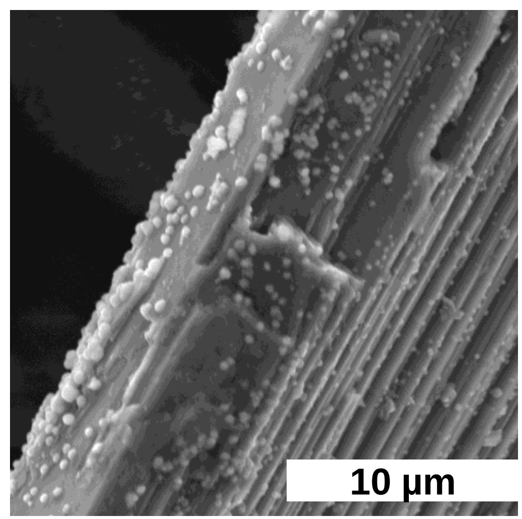

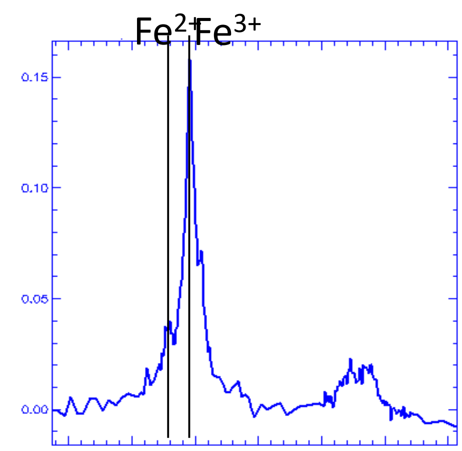

Arfvedsonite « SL 350 »
$Fe^{3+}/\Sigma Fe$ > 80 %

How to study water-rock-gas interactions at elevated T-P?

2) In situ spectroscopy: UV-Vis, Raman, IR, XAS

→ speciation, solubility

LIMITATION

- **Requires specific reaction cells**
- **Difficulties to load gas/solids**
- **Often incompatible with fluid/gas sampling**

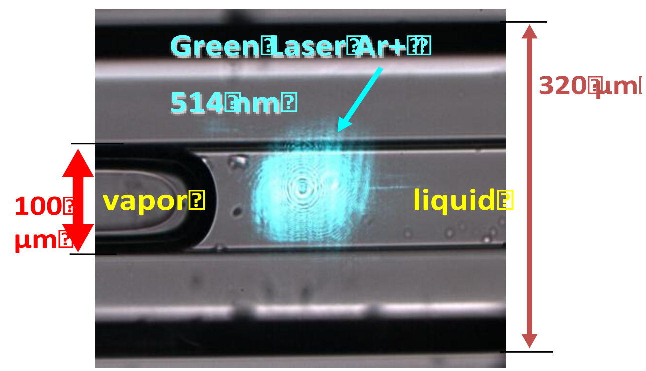

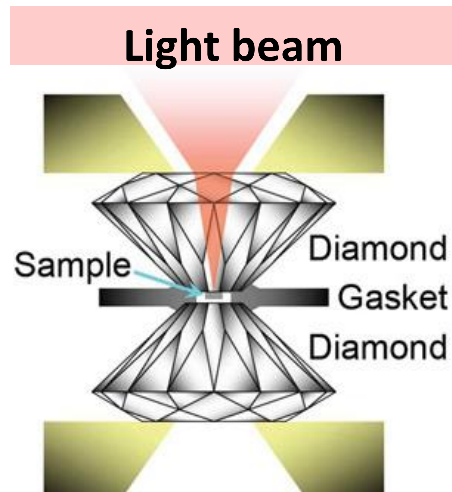

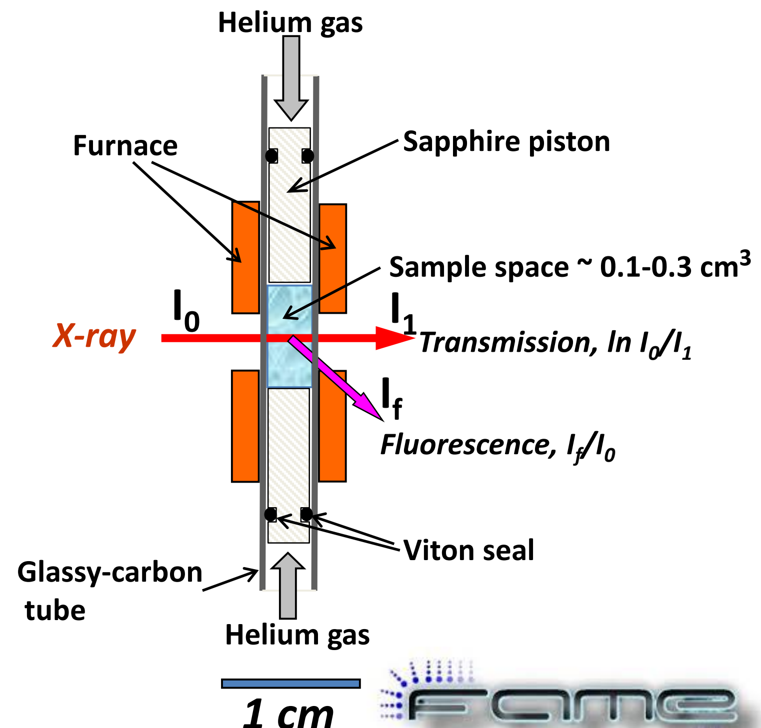

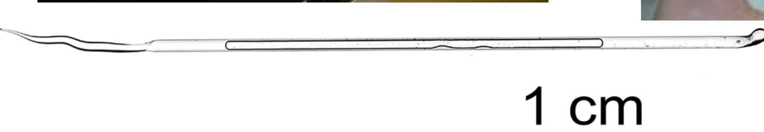

Insitu Raman spectroscopy coupled to the fused silica glass capillary technique

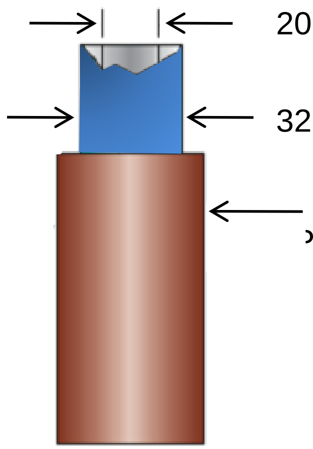

Capillary loading line

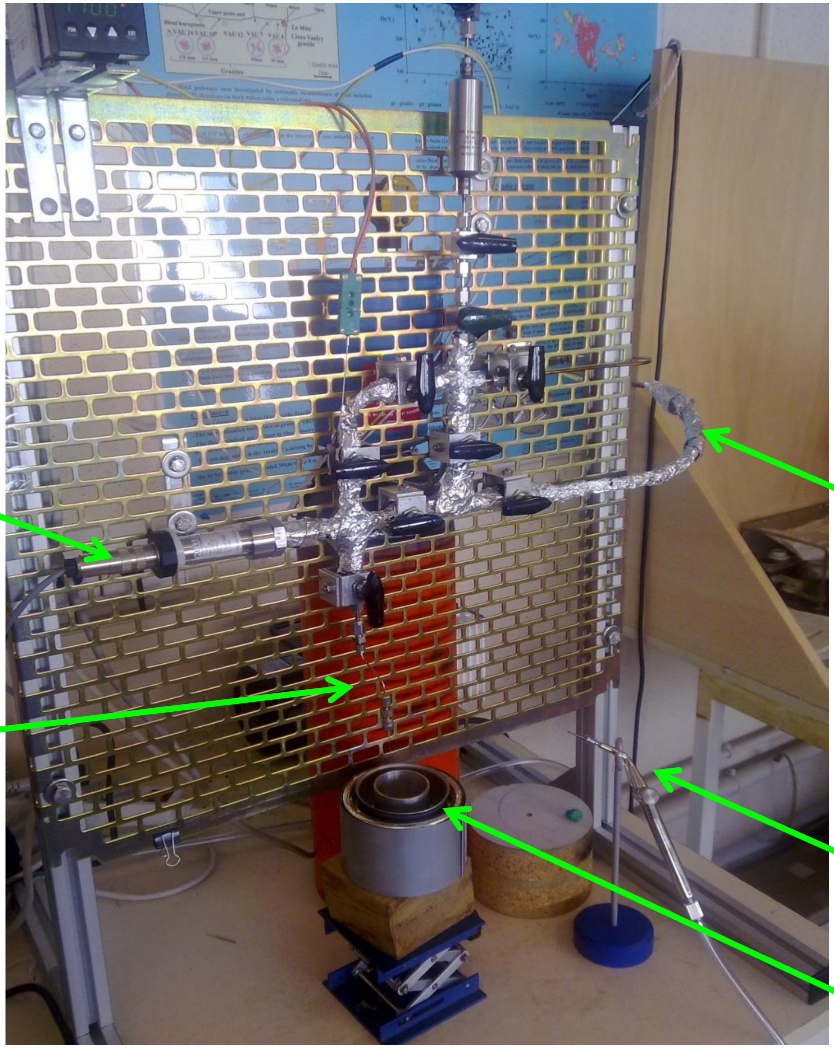

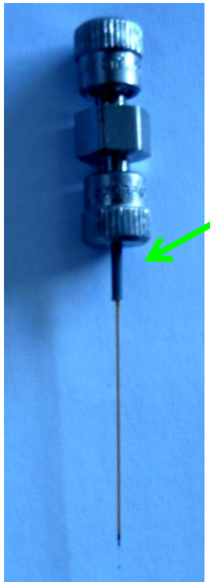

microscope (x20)
Confocal Raman
spectrometer

Heating stage® Linkam

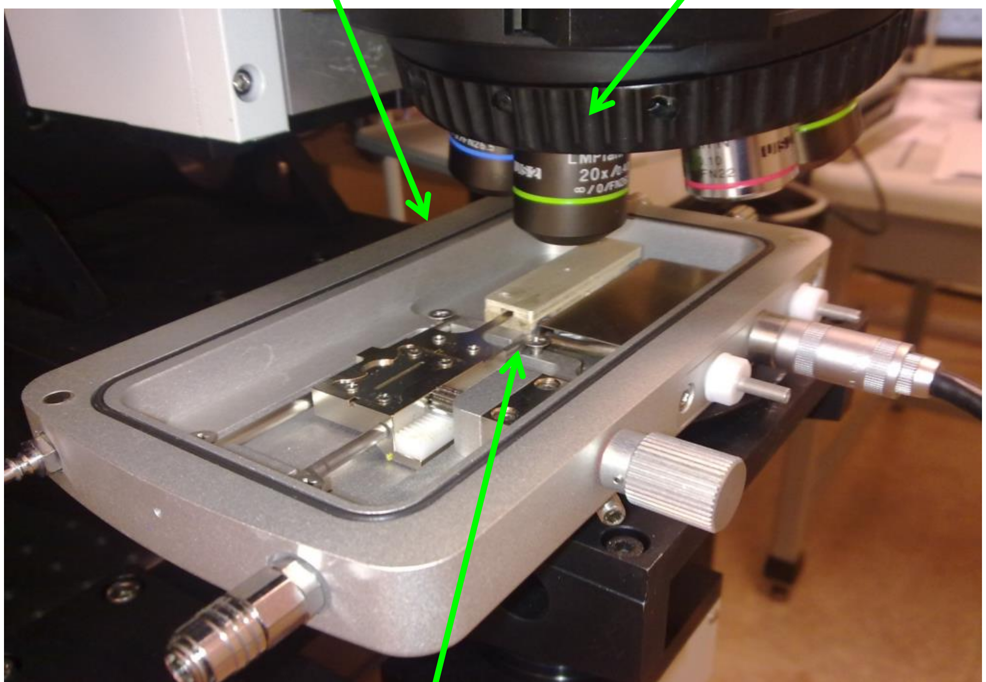

Furnace

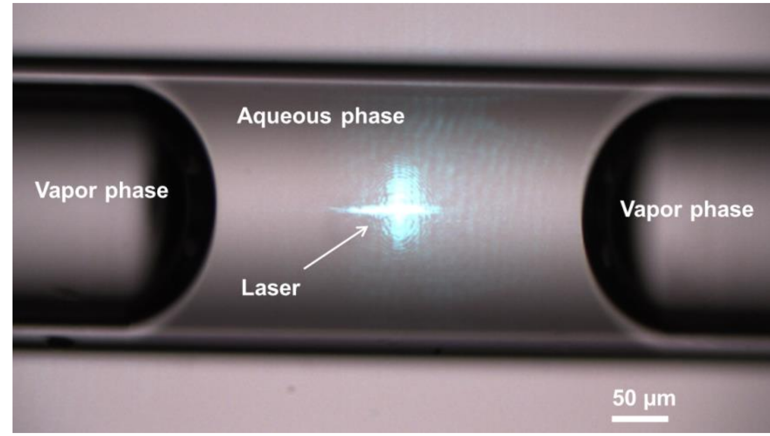

Liquid, solid (powder, or single cristal), and gas cas be loaded inside the capillary

U(VI) speciation in chloride-rich brine under hydrothermal condition

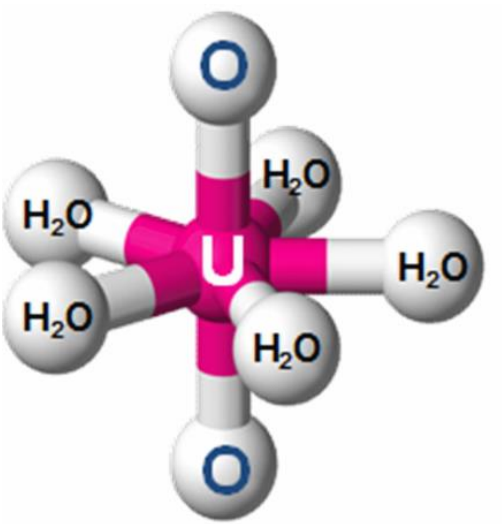

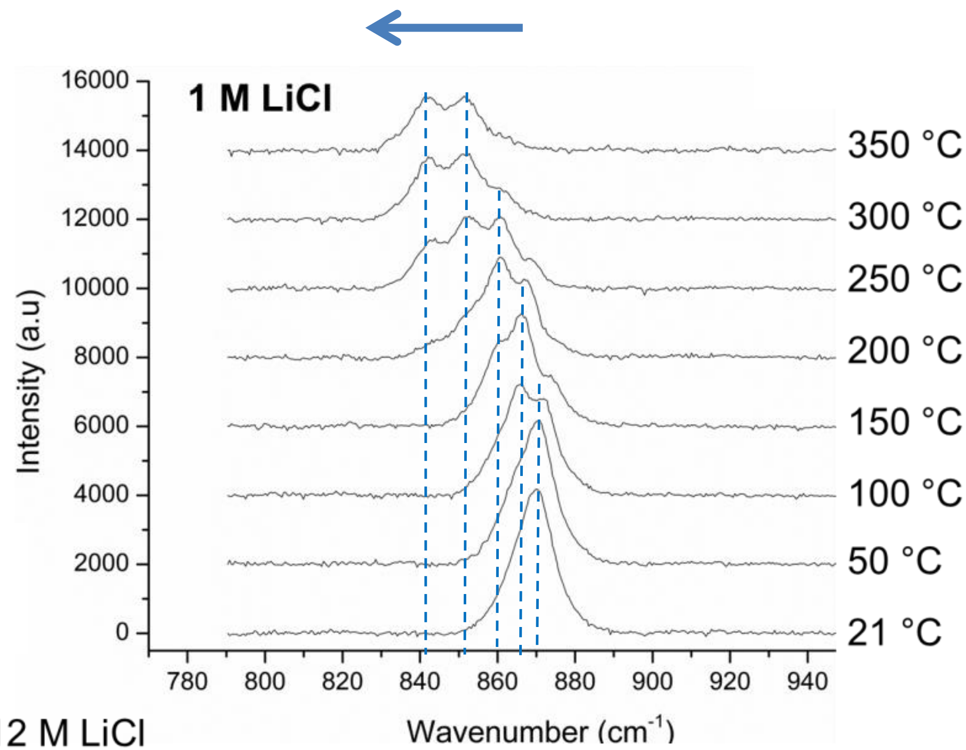

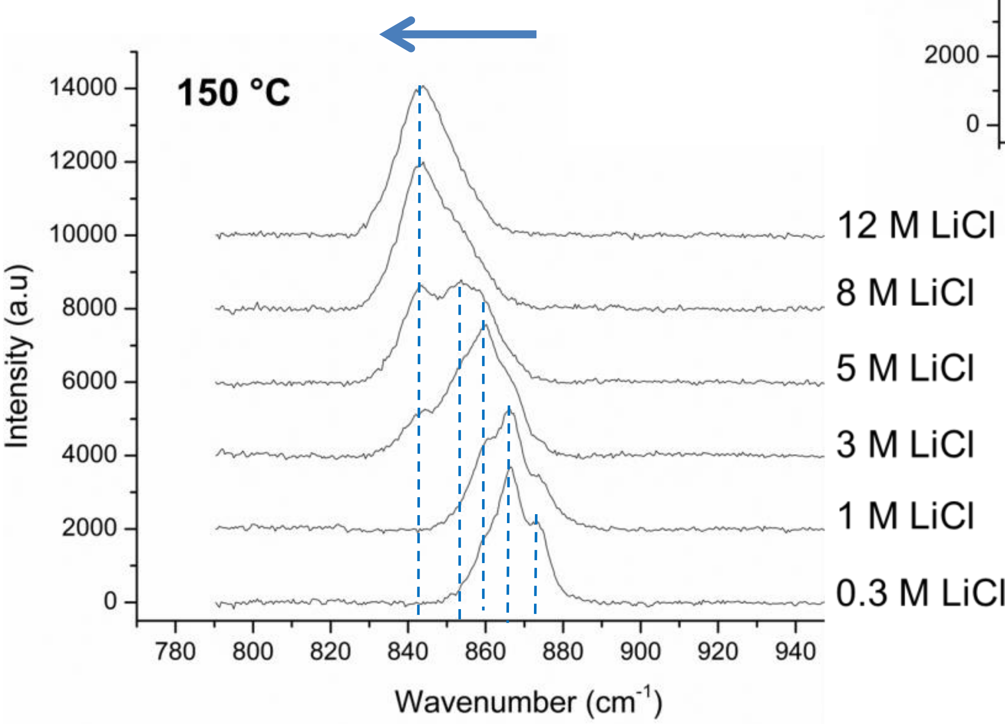

Dargent et al., 2014

U(VI) speciation in chloride-rich brine under hydrothermal condition

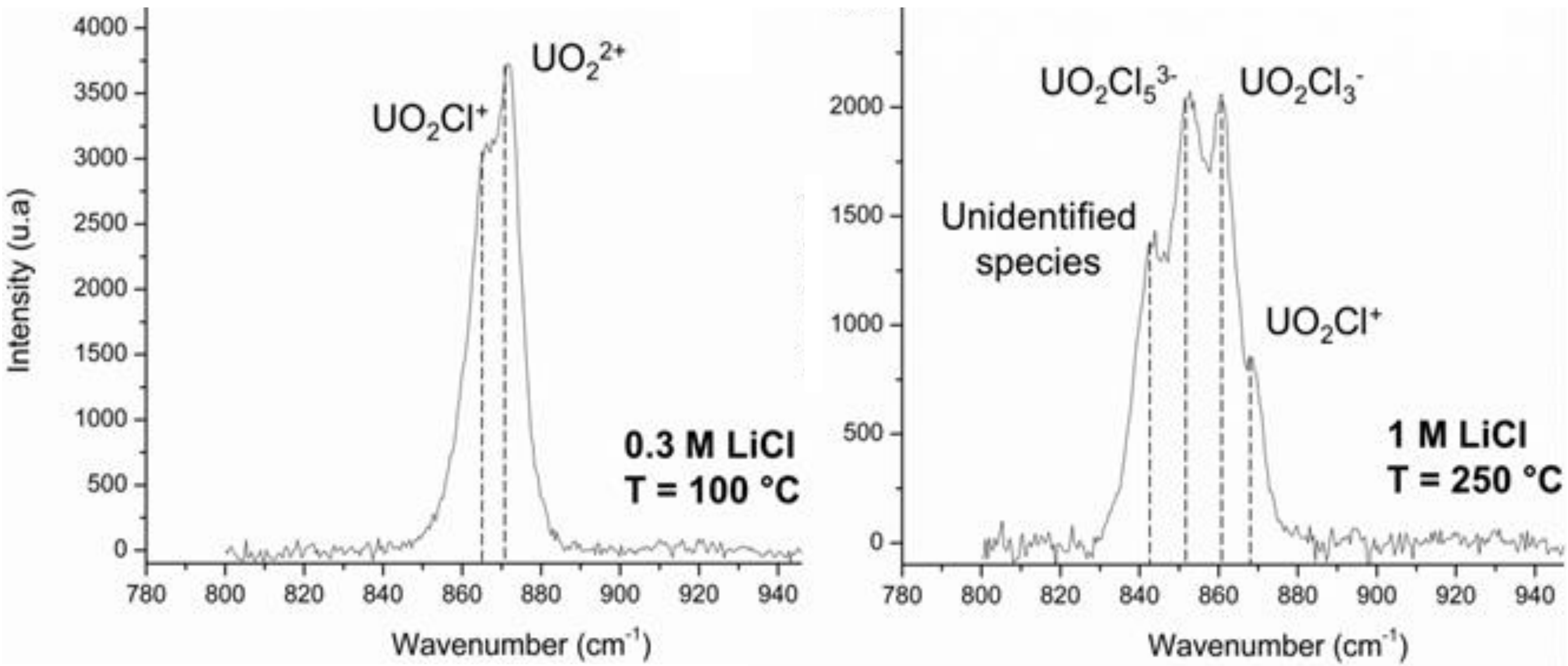

U(VI) speciation in chloride-rich brine under hydrothermal condition

Peak fitting

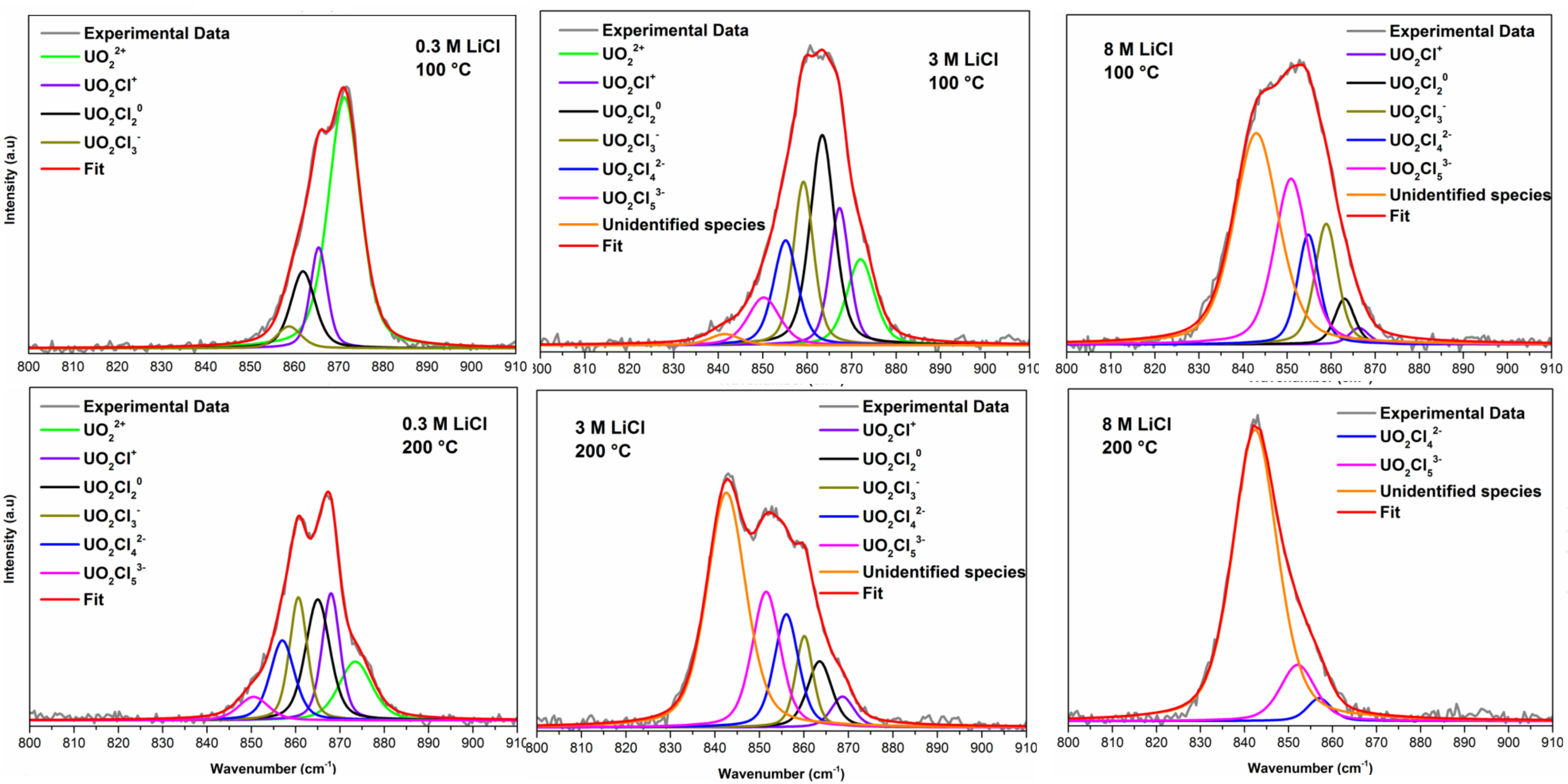

U(VI) speciation in chloride-rich brine under hydrothermal condition

$UO_2Cl_n^{2-n}{}_{(aq)} + Cl^-{}_{(aq)} = UO_2Cl_{n+1}^{1-n}{}_{(aq)}$ → $K^i_{n+1} = \frac{a^i_{UO_2Cl_{n+1}{}^{2-(n+1)}}}{a^i_{UO_2Cl_n{}^{2-n}} \times a^i_{Cl^-}}$ T_i, P_i

Tempe

$\gamma_j \times m^i_j$

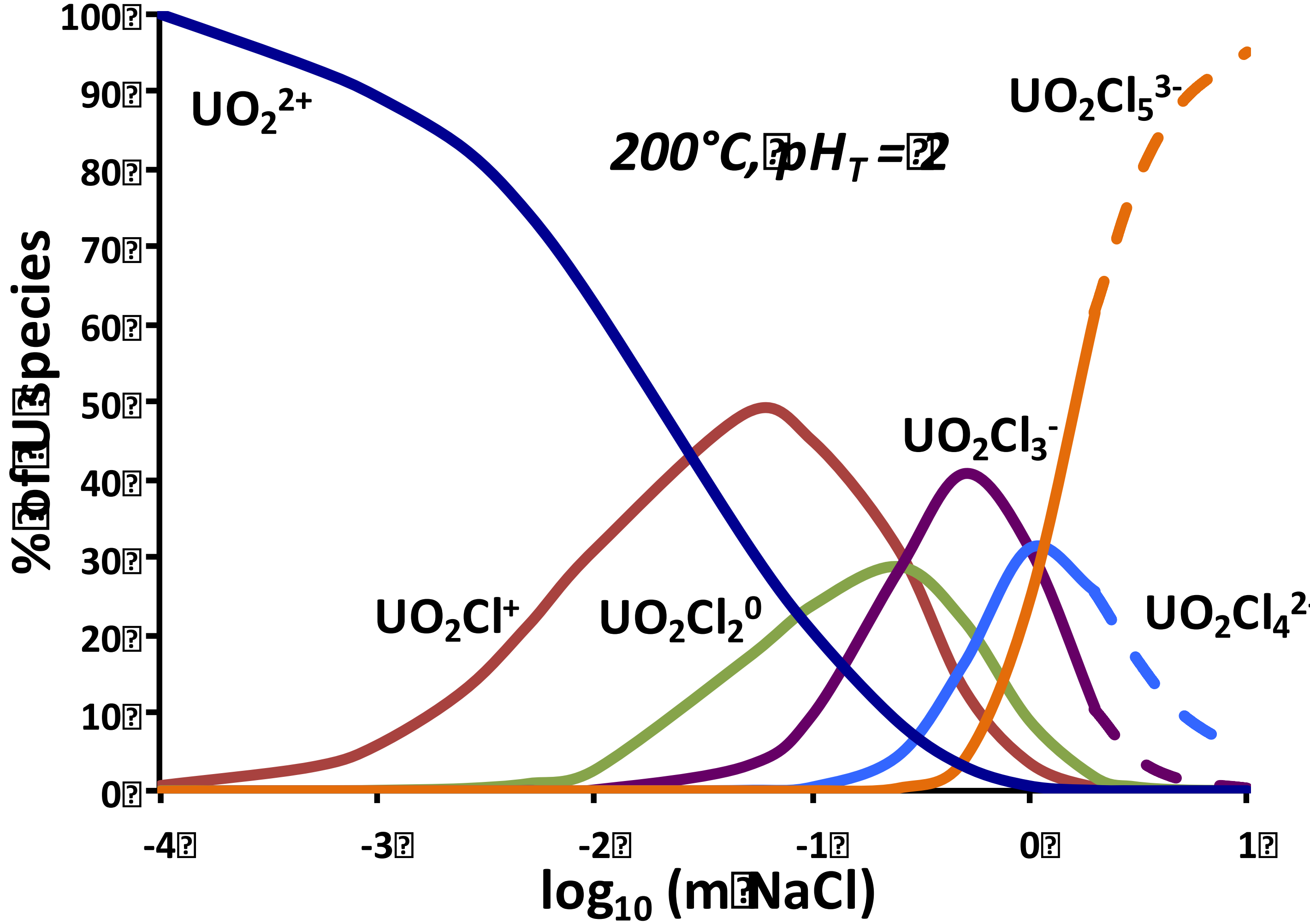

W(VI) speciation under hydrothermal condition

$HWO_4^- = H^+ + WO_4^{2-}$

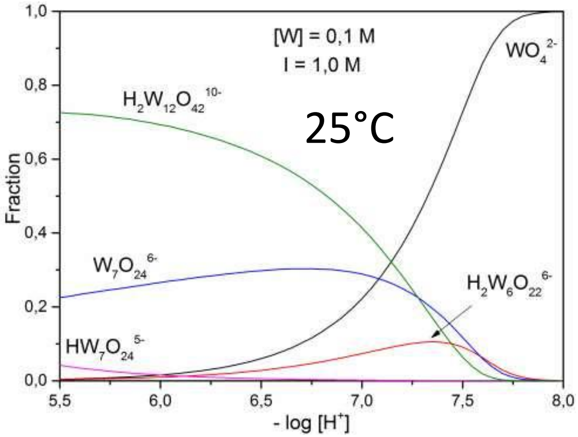

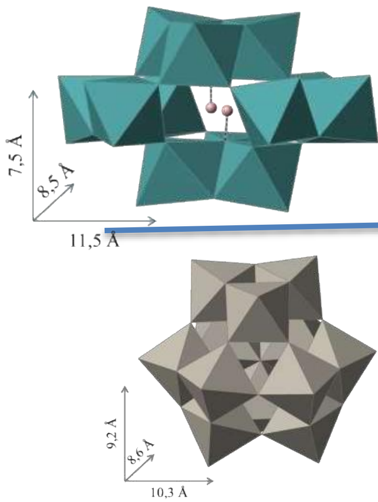

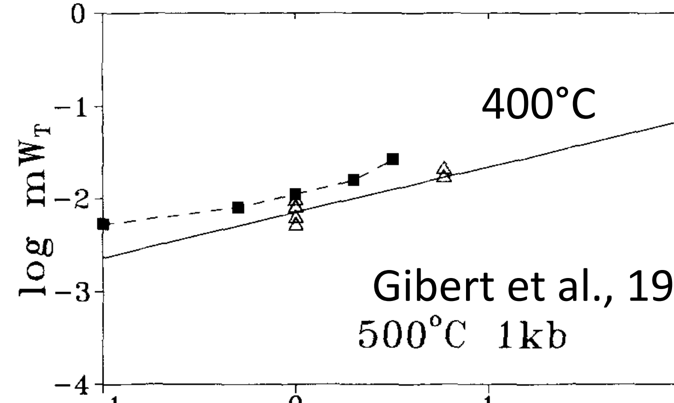

Gibert et al., 1992

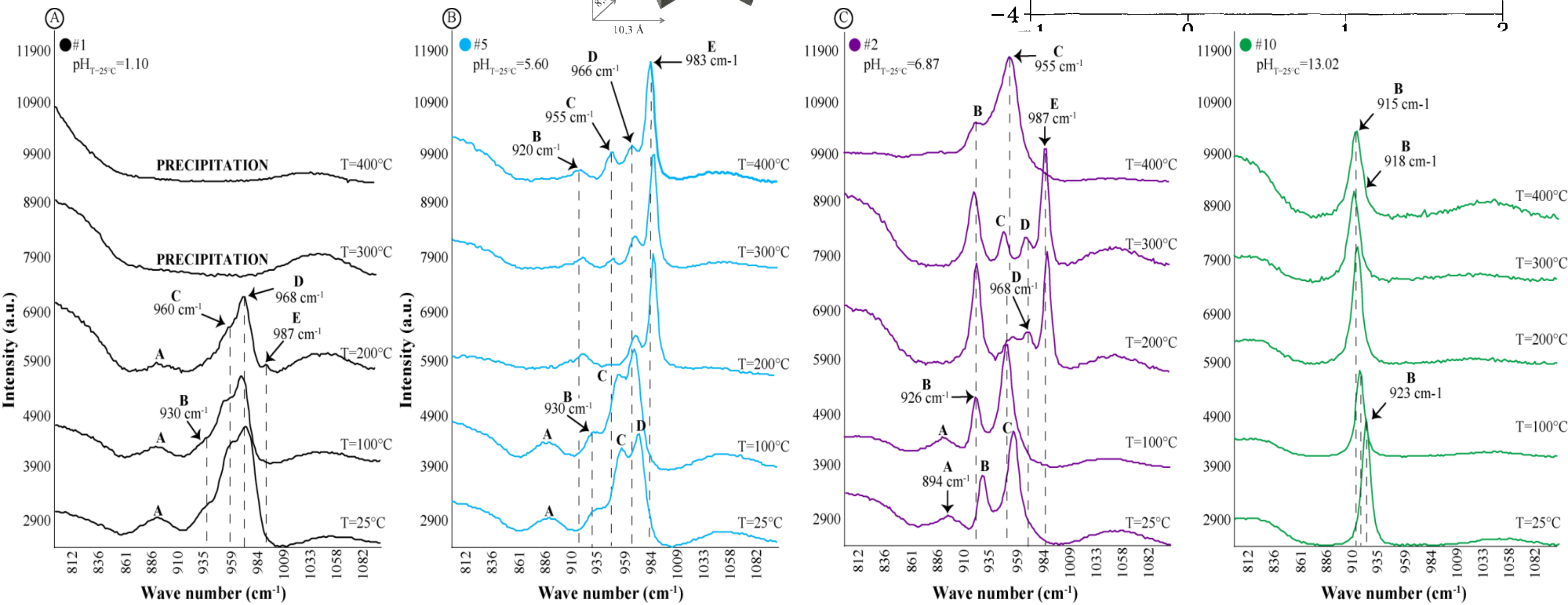

pH increases

Carocci et al., in prep

How to study water-rock-gas interactions at elevated T-P?

3) In situ potentiometry

→ **pH and redox measurement, activity of other species with selective electrodes (e.g. Na, Cd)**

LIMITATION:

Measurements are difficult to achieve

- Resistance to chemical attack
- Resistance to thermal and mechanical stress
- Stable potentials that can be resolved within few millivolts

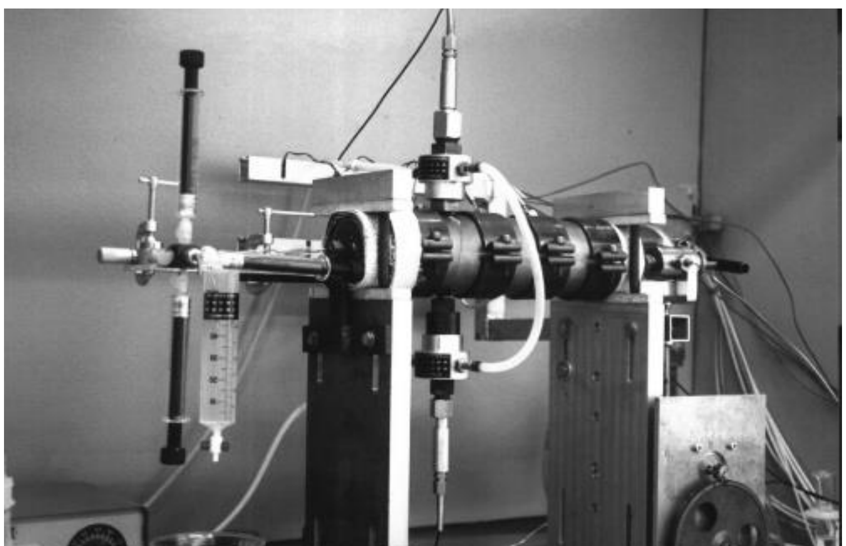

Ding and Seyfried

Glass electrode

Courtesie A. Zotov and E. Bazarkina (IGEM-RAS - Russia)

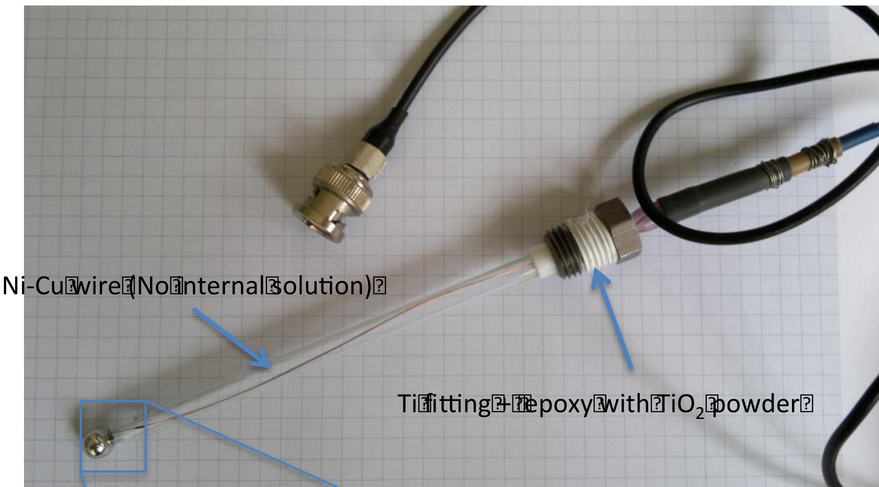

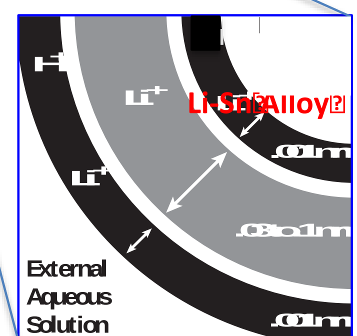

Li, Na, K interferences

ZrO_2 based pH electrode + flow through Ag/AgCl reference electrode

Combining fluid sampling + Raman spectrometry + potentiometry in a single autoclave

Fluid Sampling Autoclave

In situ Raman Spectroscopy

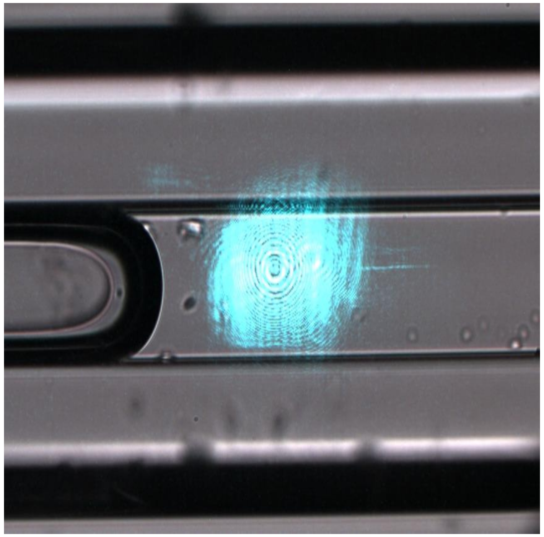

Potentiometry In situ pH measurements

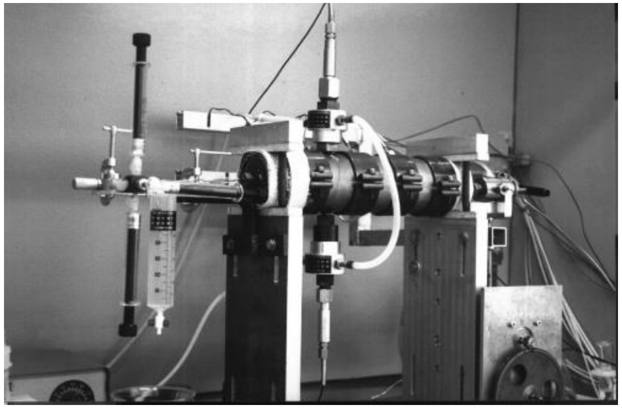

Direct measurements of CO_2 solubility and pH in NaCl hydrothermal solution up to 280 °C and 150 bar

Truche et al., 2016

Experimental setup

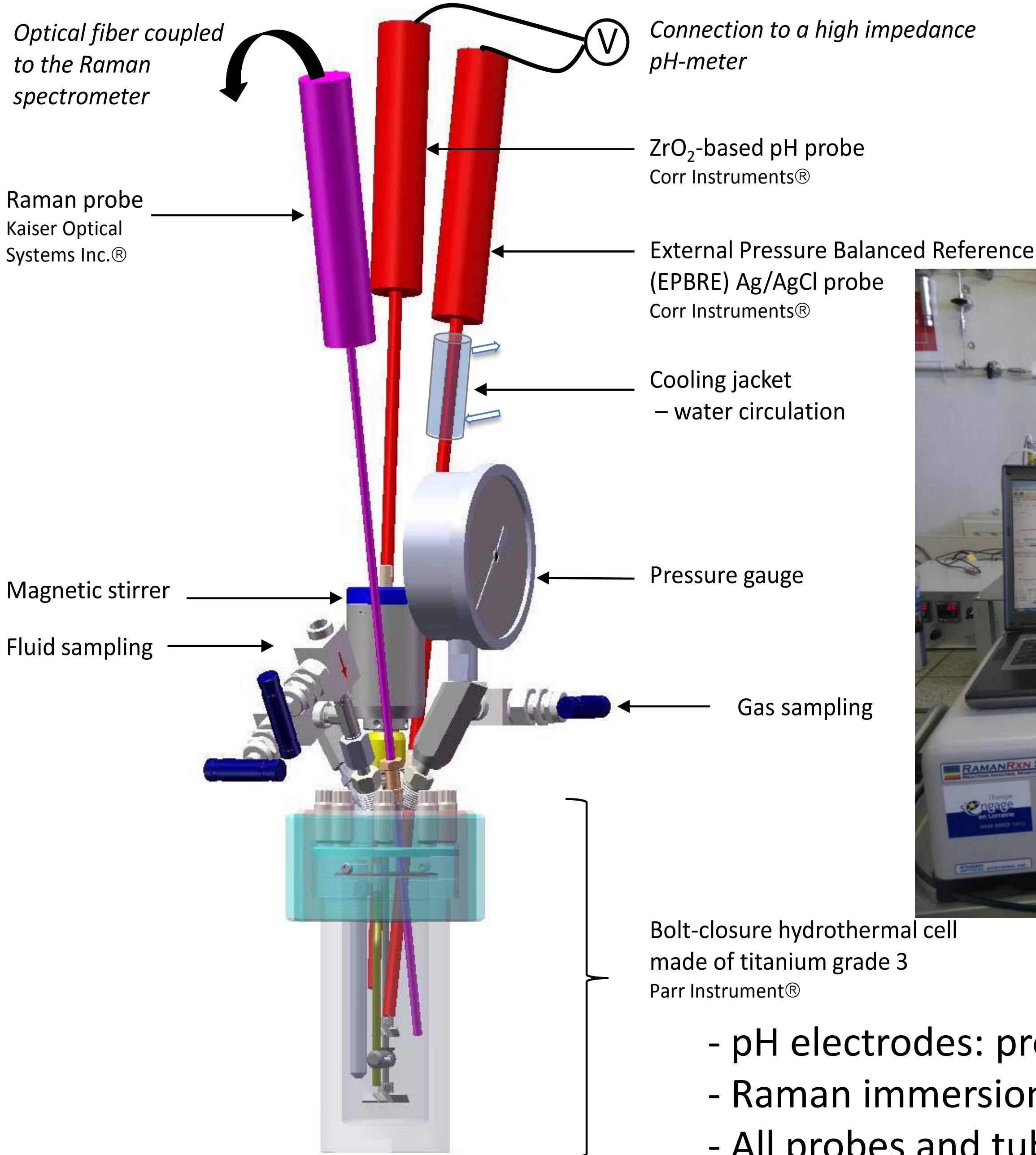

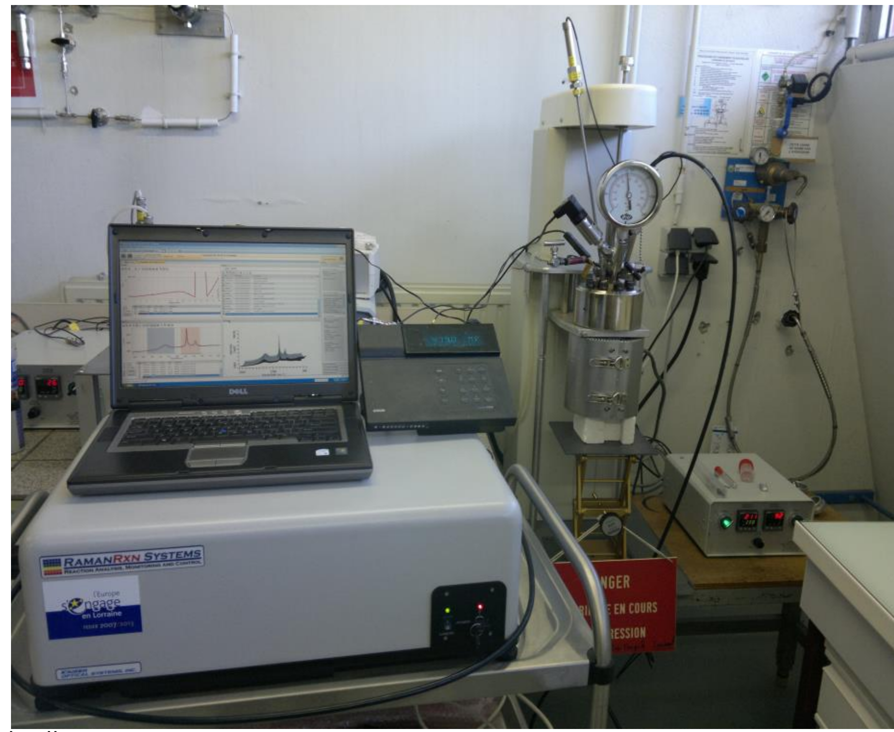

- pH electrodes: prototype from **Corr instruments**
- Raman immersion probe from **Kayser optical**
- All probes and tubing made of titanium

Dissolved CO_2 concentration measurements – Raman spectroscopy

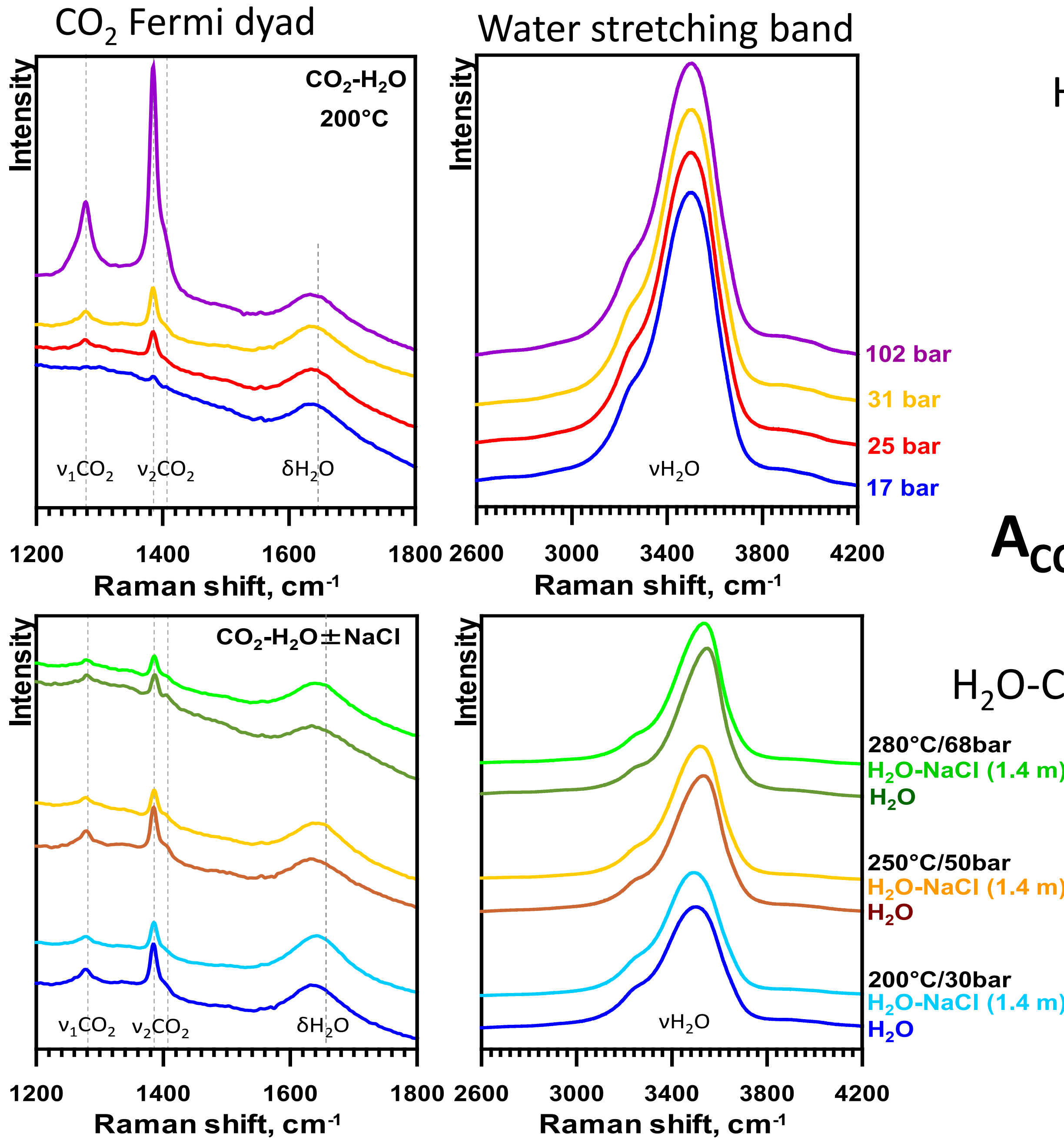

H_2O-CO_2 system

T = 200°C ,
17<P<102 bar

$$A_{CO2} = k \times [CO_{2(aq)}]$$

H_2O-CO_2 1.4 m NaCl system

200<T<280°C ,
P ≈ 50 bar

Salting out effect

Dissolved CO_2 concentration measurements – Raman spectroscopy

Calibration: gravimetric measurements as $BaCO_3$

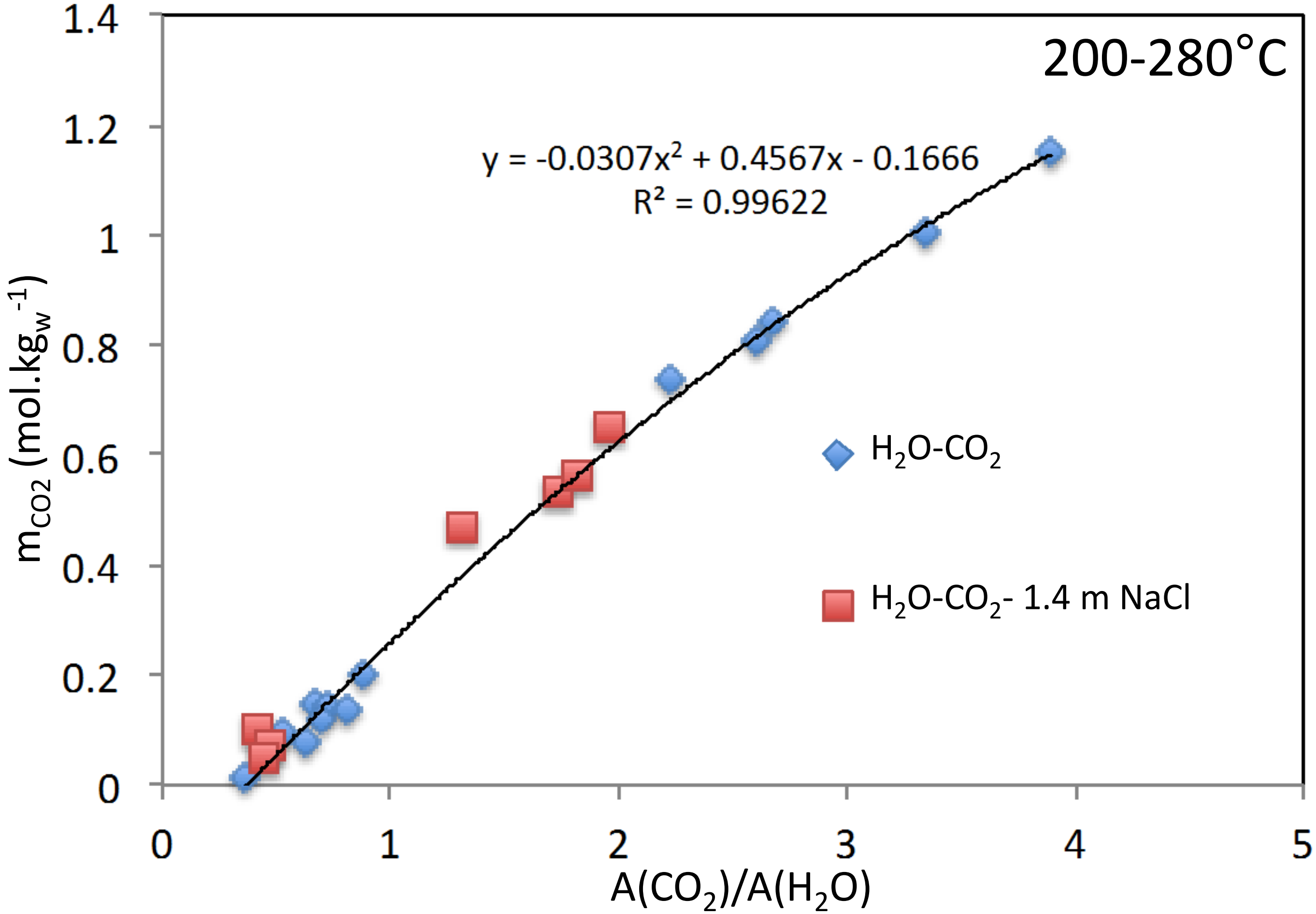

Quantification limit = 0.04 m

In-situ pH measurements

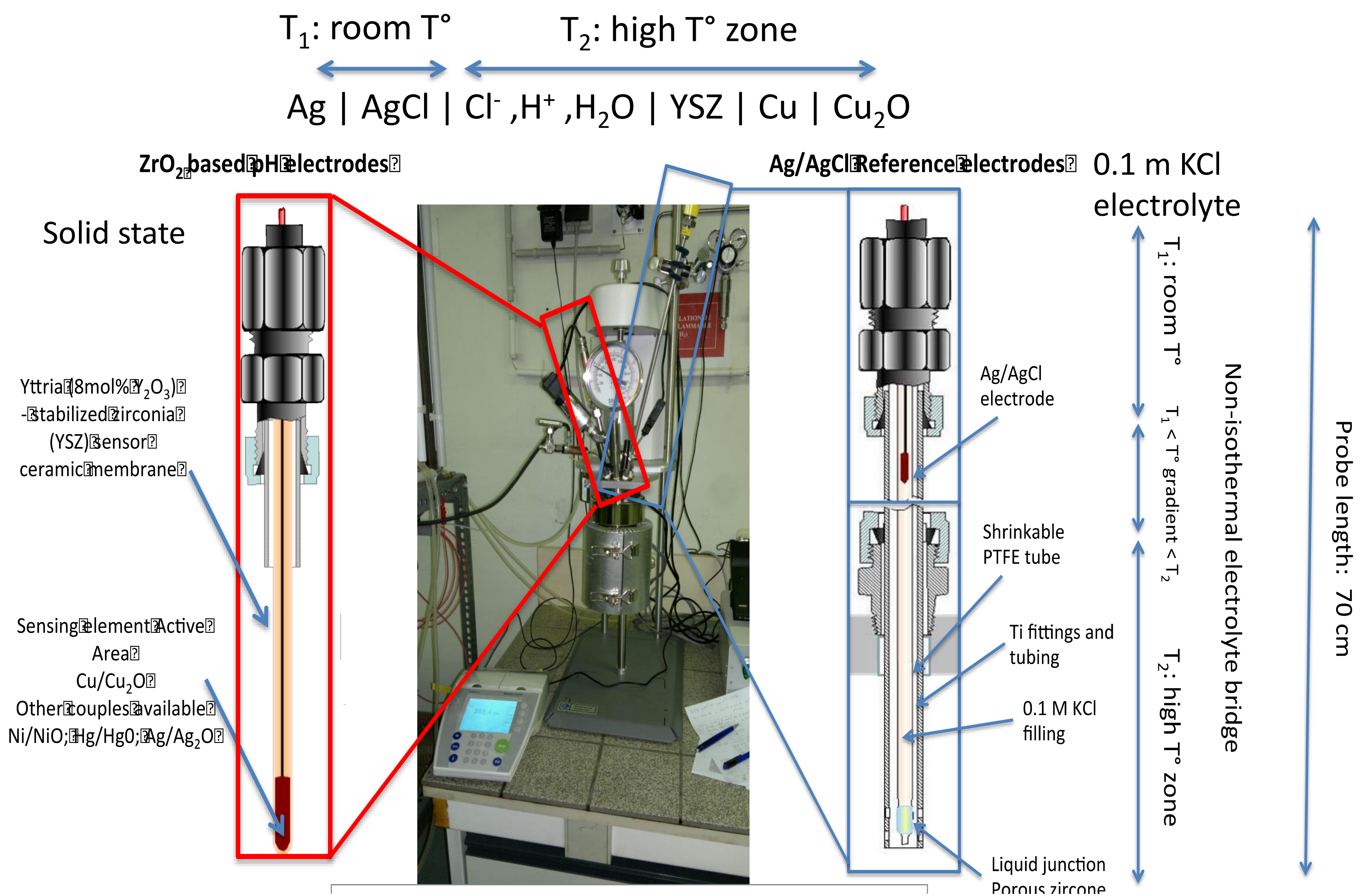

Yttria (8 mol% Y_2O_3) - stabilized zirconia (YSZ)ceramique membrane

originally described by Niedrach (1980)

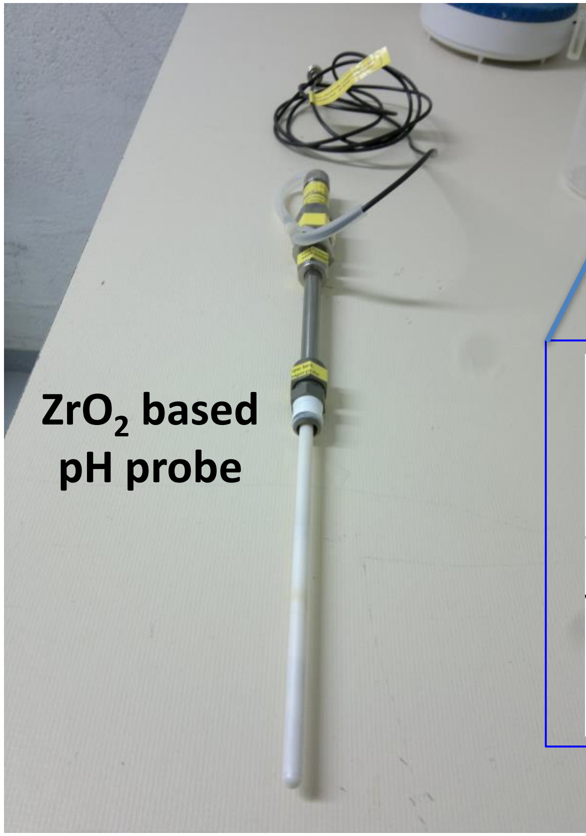

ZrO_2 based pH probe

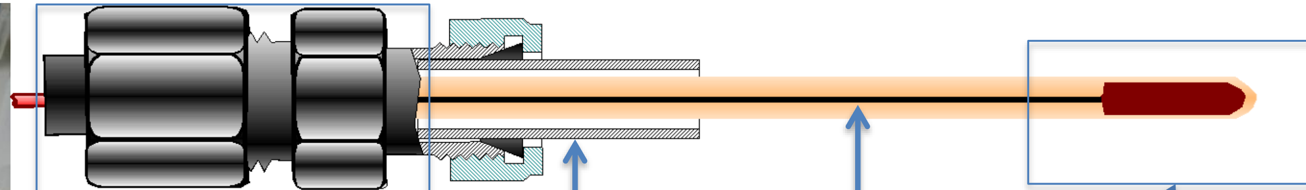

Ti tubing

Cu Conduction wire with PTFE insulation

Sensing element Active Area

Cu/Cu_2O

Other couples available

Ni/NiO; Hg/HgO; Ag/Ag_2O

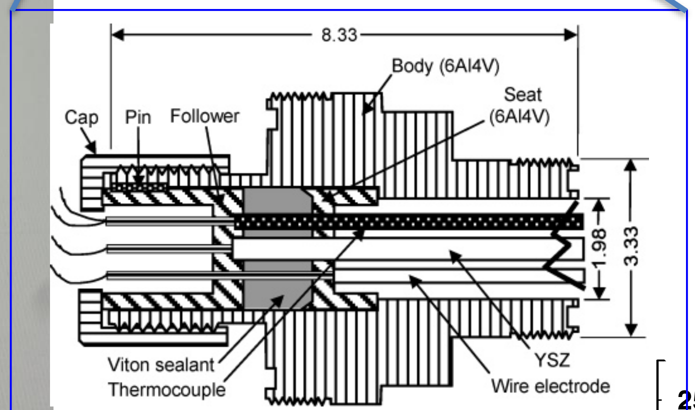

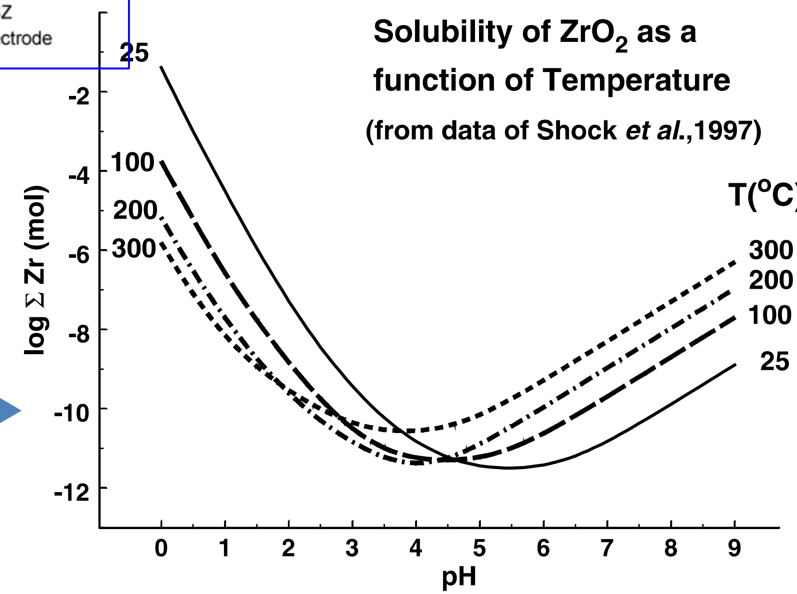

Solubility of ZrO_2 as a function of Temperature (from data of Shock *et al.*,1997)

Advantage:

- Can be use as a primary electrode
- Independent of fH_2, fO_2, Cl^-, F^-, H_2S
- Chemical stability
- Appropriate electrochemical properties
- No Na interference

ZrO_2-based pH Electrode mechanism (Mcdonald et al., 1992; Lvov et al., 2003)

1- Equilibrium at the solution side electrical potential of the ZrO_2 tube

$$V_{O}^{\cdot\cdot} + H_2O \leftrightarrow O_O + 2H^+$$

2- Equilibrium at the internal reference element

$$MO_x + xV_{O}^{\cdot\cdot} + 2xe^- \leftrightarrow M + xO_O$$

- if:
  - i) oxygen vacancy activity is constant throughout the ceramic and,
  - ii) measurements are carried out potentiometrically (zero current through the membrane
- Then the sensor potential is given by:

$$MO_x + 2xH^+ + 2xe^- \leftrightarrow M + xH_2O$$

$$\Rightarrow \quad E = E^0_{M/MO_x} - \left(\frac{2.303RT}{2F}\right)\log(a_{H_2O}) - \left(\frac{2.303RT}{F}\right)pH$$

(1) the potential of the YSZ sensor should be Nernstian with respect to pH
(2) The accuracy significantly depends on the choice of the metal/metal oxide redox couple, and
(3) no property of the ceramic membrane appears in any of the terms

Quality of the zirconia membrane !!!

The optimum composition of 8 mol% Y_2O_3

- remains cubic and avoids fracturing due to a volume change in phase transition
- electrically responsive
- few ppm of redox-active impurities in the ZrO_2 ceramics, such as Fe or Ti, may seriously alter the oxygen diffusivity

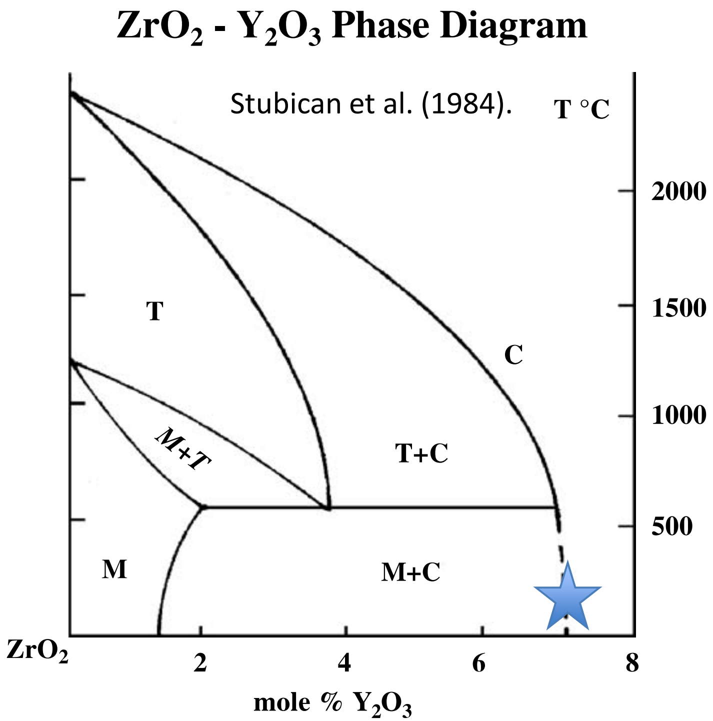

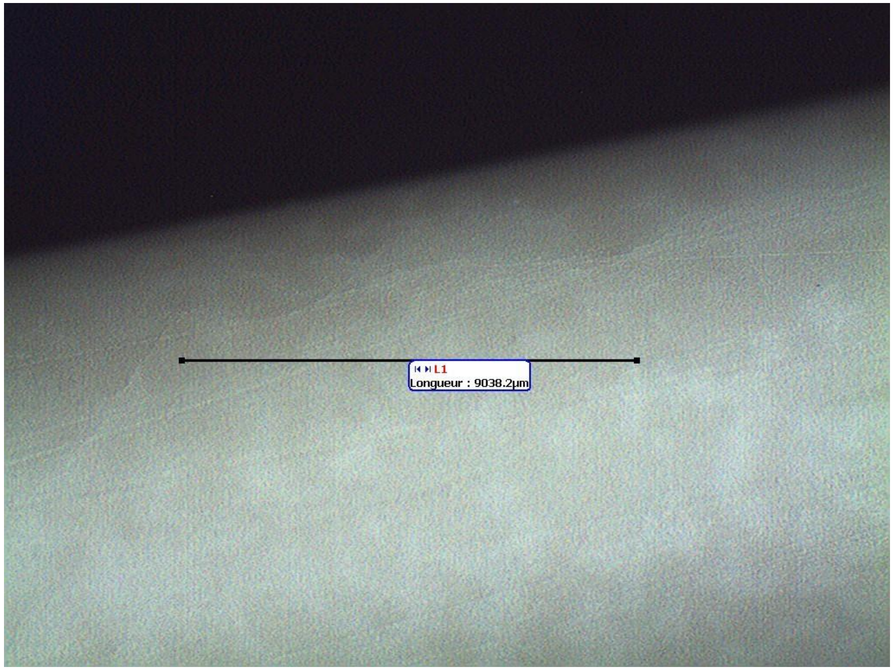

Ag/AgCl Reference electrodes: the key point

External pressure-balanced Ag/AgCl reference electrode

- Pressure balancing obtained **a flexible PTFE** tube → avoid **streaming potential**
- **Ag/AgCl** redox couple in the cold part → avoid **hydrolysis and reduction** at high T
- **Constant thermal gradient along the probe → constant liquid junction potential**

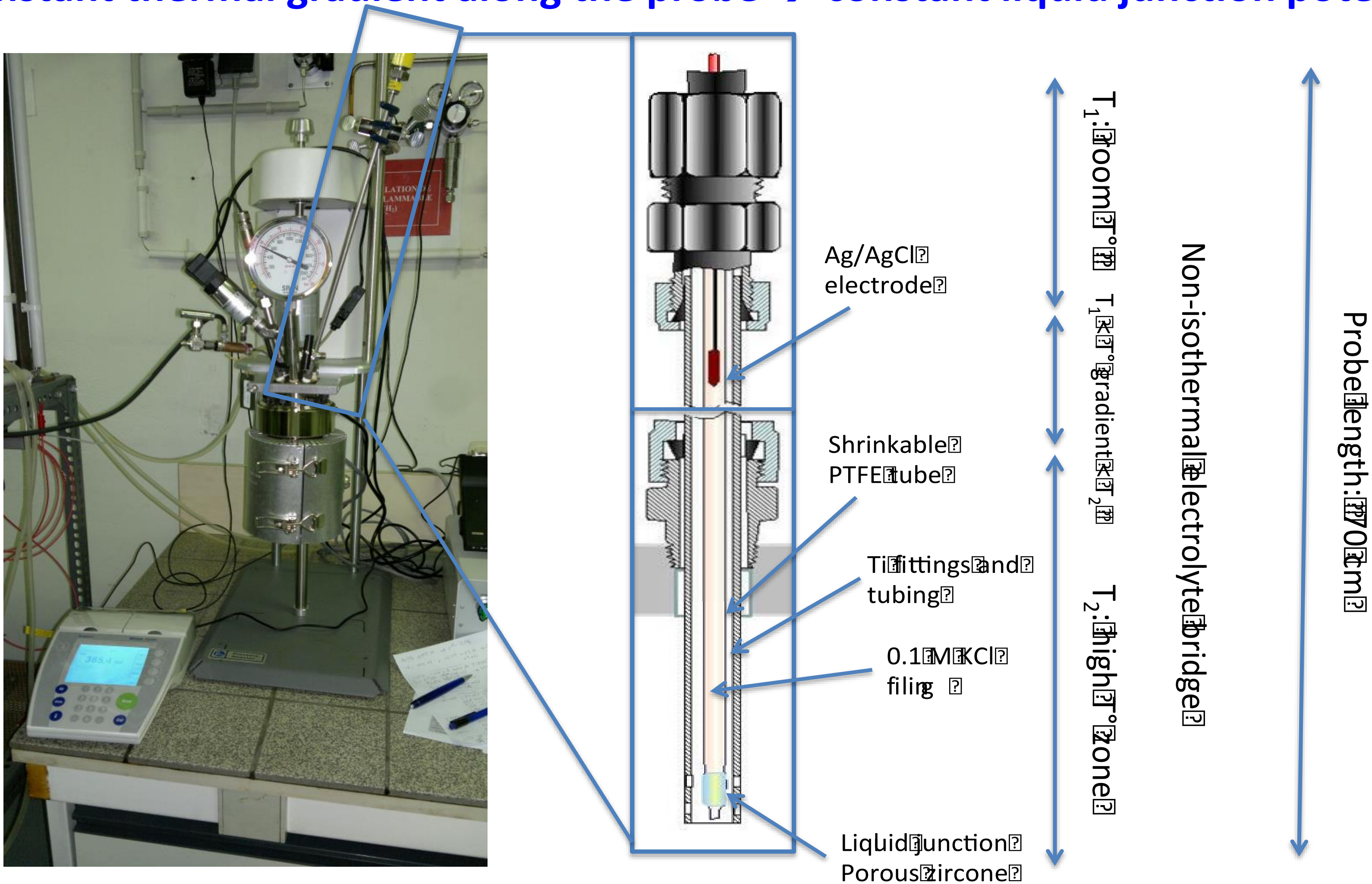

pH probes calibration

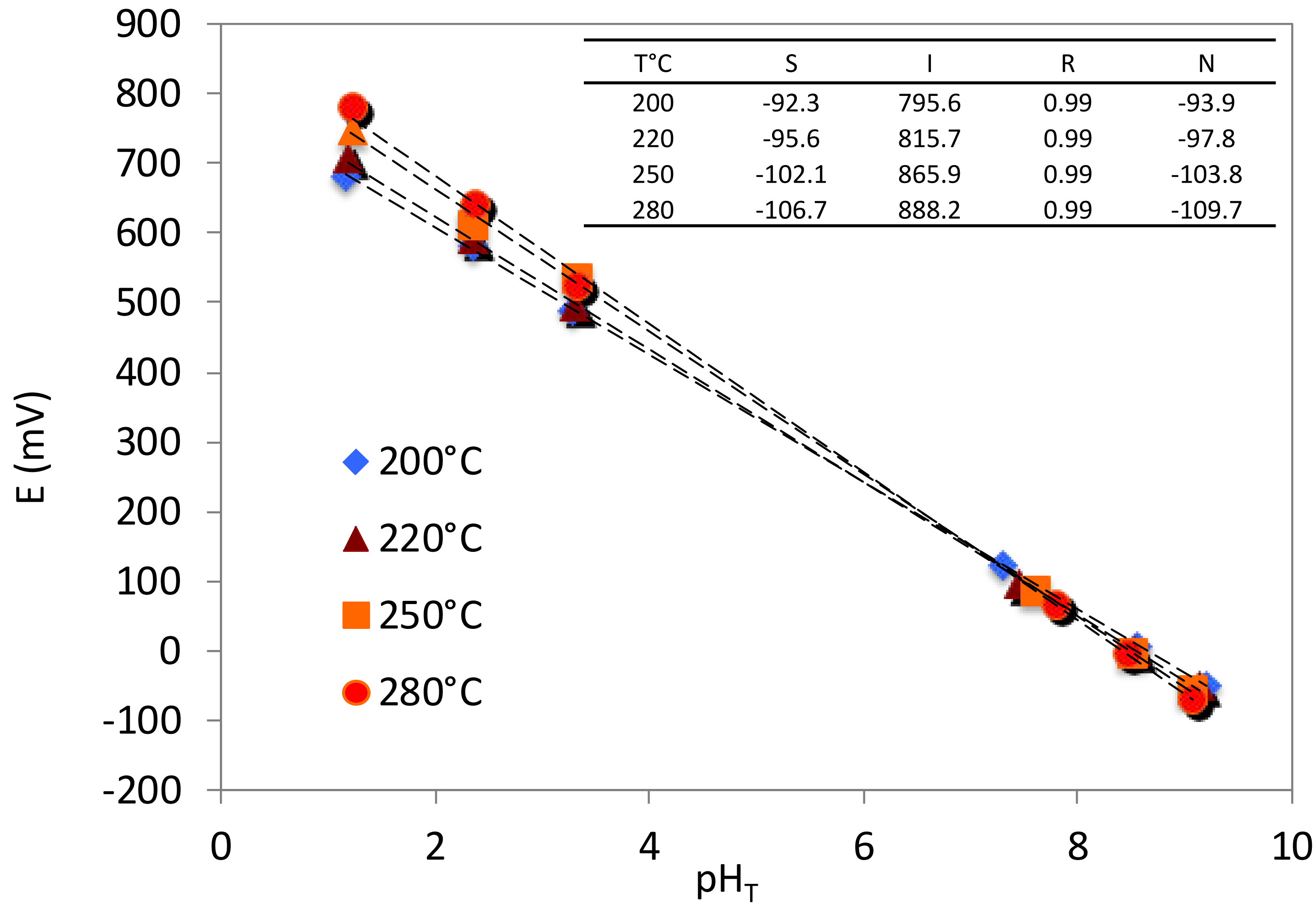

T°C	S	I	R	N
200	-92.3	795.6	0.99	-93.9
220	-95.6	815.7	0.99	-97.8
250	-102.1	865.9	0.99	-103.8
280	-106.7	888.2	0.99	-109.7

pH buffers:

- H_2SO_4
- KPO_4/Na_2HPO_4
- $Na_2B_4O_7$
- NaOH

Perfect Nernstian response up to 280°C

Accuracy: 0.05 pH unit

pH probes calibration: effect of salinity (up to 3m NaCl)

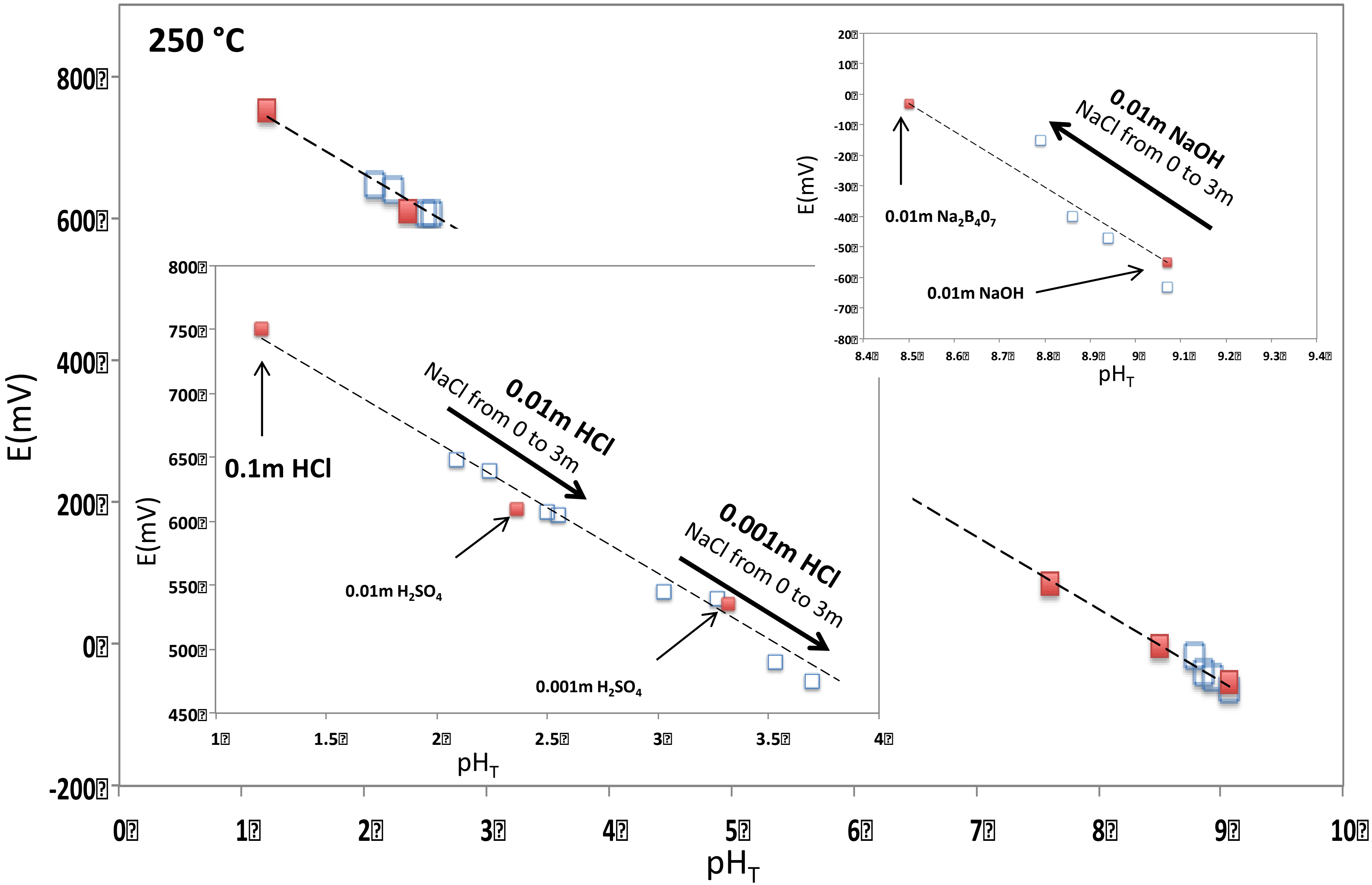

Salinity has no effect on the calibration line

In situ pH in the CO_2-H_2O system

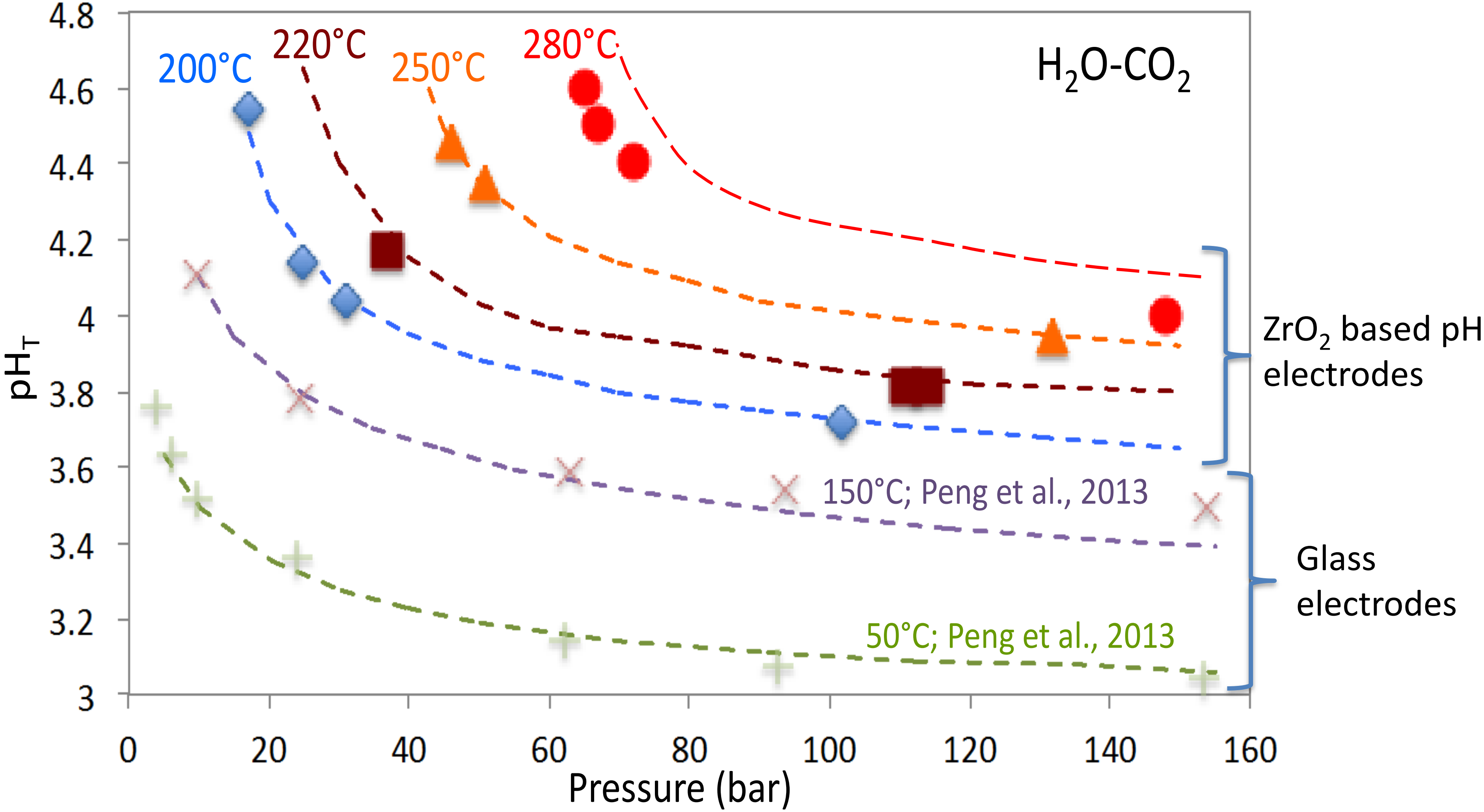

In situ pH in the CO_2-NaCl-H_2O system

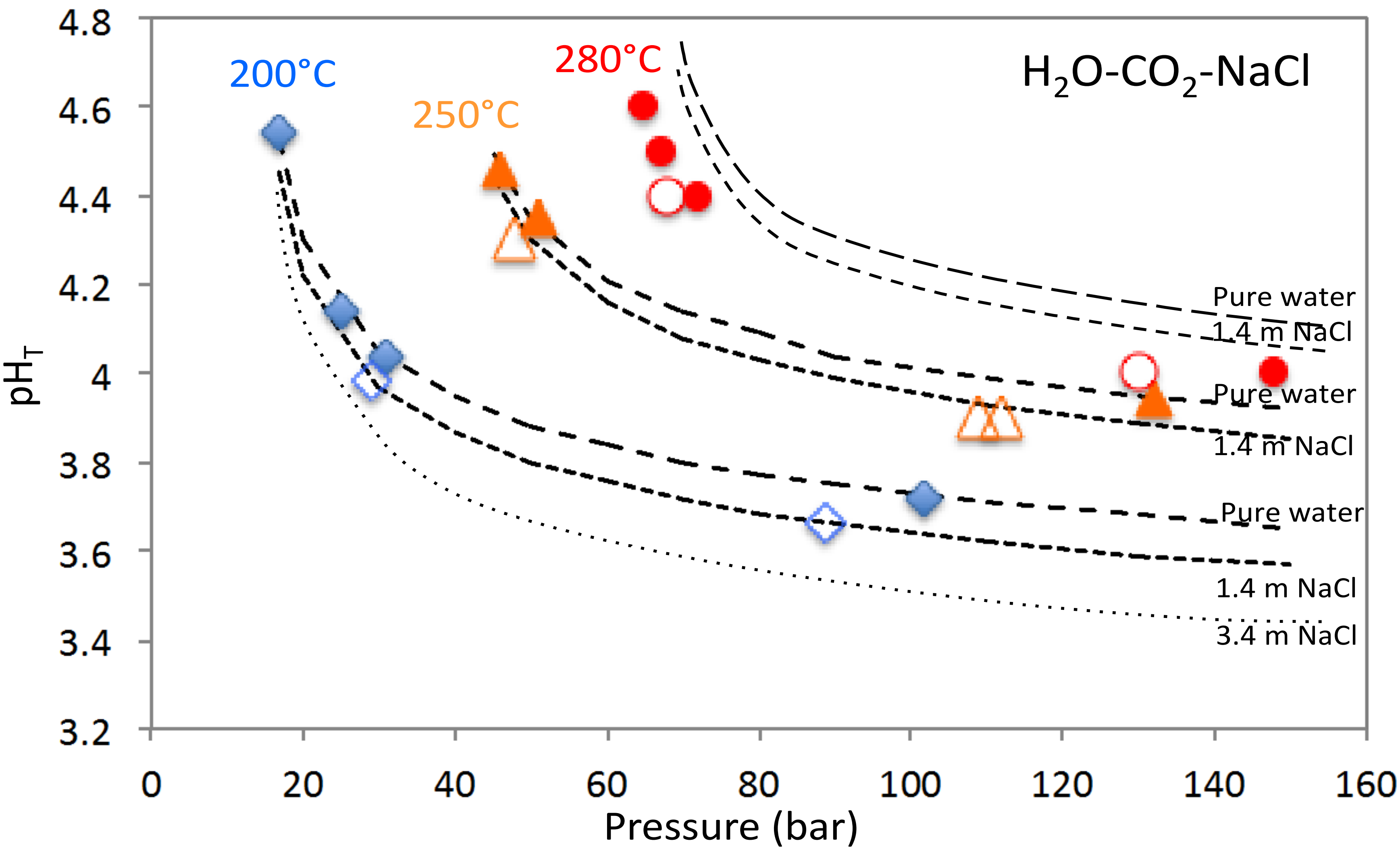

- at constant P: increase [NaCl] → decrease pH

Pitzer model based on carefully revised parameters – ready to use with Phreeqc

All the Pitzer parameters are available on Truche et al. (2015), GCA, 177, 238-253

A pitzer model ready to use with Phreeqc code

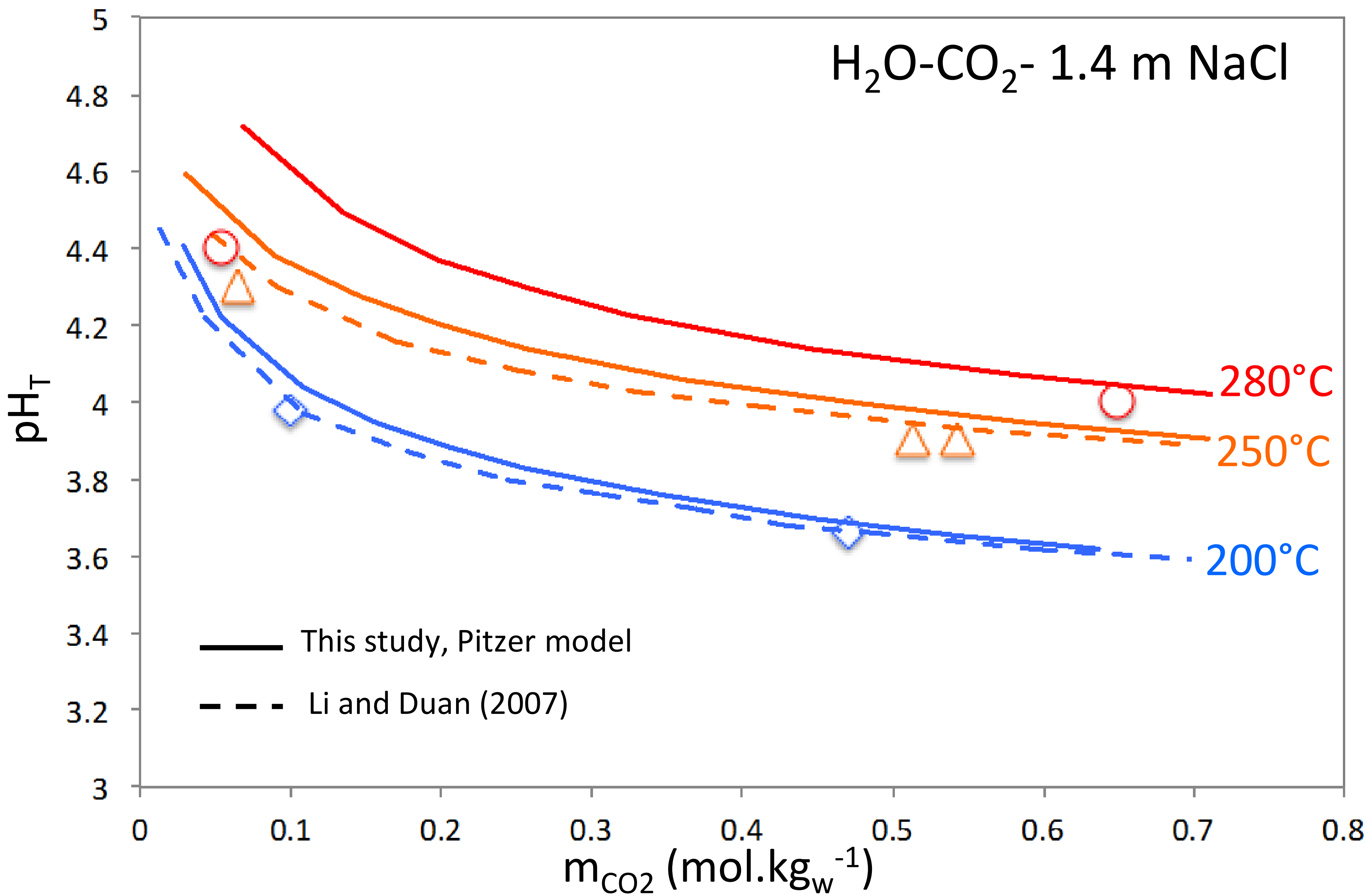

All the Pitzer parameters are available on Truche et al. (2015), GCA, 177, 238-253

CONCLUSION

- Combination of different techniques is essential to gain full insight into a reaction process
- Recent advance in spectroscopy allow miniaturization and coupling with classical techniques (e.g. batch autoclave)
- Advises:

- workshop support required,

- blank experiments of prior importance

- take into consideration artefacts due to metastability (or reversibility), kinetics (or steady states), catalysis (construction material usually not inert)

- know well the weak point of the technique you using

- do not leave the others the opportunity to model/interpret your data → do it yourself!

- but…be open minded and curious to you surrounding world!

THANKS FOR YOUR ATTENTION

Any questions?